minerals

MDPI

Article

Lithofacies Characteristics of Continental Lacustrine Fine-Grained Sedimentary Rocks and Their Coupling Relationship with Sedimentary Environments: Insights from the Shahejie Formation, Dongying Sag

Hao Guo, Juye Shi *, Shaopeng Fu, Zitong Liu, Linhong Cai and Siyuan Yin

School of Energy Resources, China University of Geosciences (Beijing), Beijing 100083, China; 1006210331@email.cugb.edu.cn (H.G.); 1006210414@email.cugb.edu.cn (S.F.); 1006210532@email.cugb.edu.cn (Z.L.); 1006210215@email.cugb.edu.cn (L.C.); 1006210420@email.cugb.edu.cn (S.Y.)
* Correspondence: shijuye@cugb.edu.cn

Abstract: Lacustrine fine-grained sedimentary rocks in the Dongying Sag of the Bohai Bay Basin in China exhibit significant potential for hydrocarbon exploration. This study investigates the lithofacies types and sedimentary evolution of the Paleogene Shahejie Formation's lower third member (Es3l) and upper fourth member (Es4u), integrating petrological and geochemical analyses to explore the relationship between lithofacies characteristics and sedimentary environments. The results show that the fine-grained sedimentary rocks in the study area can be classified into 18 lithofacies, with seven principal ones, including organic-rich laminated carbonate fine-grained mixed sedimentary rock lithofacies and organic-rich laminated limestone lithofacies. In conjunction with analyses of vertical changes in geochemical proxies such as paleoclimate (e.g., CIA, Na/Al), paleoproductivity (e.g., Ba), paleosalinity (e.g., Sr/Ba), paleo-redox conditions (e.g., V/Sc, V/V + Ni), and terrigenous detrital influx (e.g., Al, Ti), five stages are delineated from bottom to top. These stages demonstrate a general transition from an arid to humid paleoclimate, a steady increase in paleoproductivity, a gradual decrease in paleosalinity, an overall reducing water body environment, and an increasing trend of terrestrial detrital input. This study demonstrates that the abundance of organic matter is primarily influenced by paleoproductivity and paleo-redox conditions. The variations in rock components are predominantly influenced by paleoclimate, and sedimentary structures are affected by the depth of the lake basin. Special depositional events, such as storm events in Stage II, have significantly impacted the abundance of organic matter, rock components, and sedimentary structures by disturbing the water column and disrupting the reducing conditions at the lake bottom. The present study offers crucial insights into the genesis mechanisms of continental lacustrine fine-grained sedimentary rocks, facilitates the prediction of lithofacies distribution, and advances the exploration of China's shale oil resources in lacustrine environments.

Keywords: fine-grained sedimentary rocks; lithofacies characteristics; sedimentary environment; Dongying Sag; Shahejie Formation

Citation: Guo, H.; Shi, J.; Fu, S.; Liu, Z.; Cai, L.; Yin, S. Lithofacies Characteristics of Continental Lacustrine Fine-Grained Sedimentary Rocks and Their Coupling Relationship with Sedimentary Environments: Insights from the Shahejie Formation, Dongying Sag. *Minerals* **2024**, *14*, 479. https://doi.org/ 10.3390/min14050479

Academic Editors: Luca Aldega, Junwen Peng and Xiongqi Pang

Received: 25 March 2024
Revised: 19 April 2024
Accepted: 26 April 2024
Published: 30 April 2024

1. Introduction

Fine-grained sedimentary rocks hold a significant position in the spectrum of sedimentary rocks, comprising about two-thirds of this category [1]. It is widely believed that these fine-grained sedimentary rocks are primarily composed of particles smaller than 62.5 µm, including clay minerals, quartz, feldspars, carbonates, and organic matter [2]. Notably, those developed in deep-water environments and rich in organic matter are key source rocks for hydrocarbon generation [3–5]. However, due to the small size of mineral particles in fine-grained sedimentary rocks, their susceptibility to weathering, the subtlety of their sedimentary structures, and constraints in experimental conditions, the study of these rocks

has long been overlooked [6,7]. In recent years, there has been a significant acceleration in the global exploration and development of shale oil and gas. This can be attributed to the rise of unconventional oil and gas exploration, as well as the successful exploitation of North American shale resources [8–10]. Consequently, fine-grained sedimentary rocks, especially those rich in organic matter and developed in deep-water environments, have garnered increasing attention. China's shale oil resources have tremendous potential. In the Bohai Bay Basin's Jiyang Depression [11,12], the Nanxiang Basin's Biyang Depression [13,14], the Songliao Basin [15], and the Santanghu Basin [16], shale oil flow has been achieved to varying degrees.

Current research on the lithofacies of fine-grained sedimentary rocks has predominantly focused on marine deposits. For instance, Milliken et al. (2012) categorized these based on a ternary classification of intrabasinal and extrabasinal particles [17]. Researchers like Wang et al. (2013) and Jiang et al. (2016) have classified lithofacies based on TOC (total organic carbon) content and mineral composition [18,19]. Loucks et al. (2007) have employed a classification system based on mineralogy, structure, and biological features [20]. Simenson et al. (2010) and Zou et al. (2010) have named these rocks by combining mineral, structural, and biological characteristics and color attributes [21,22]. Liang et al. (2012) and Abouelresh et al. (2012) have considered lamination, structure, biotic communities, and mineral composition as criteria for differentiating marine shale lithofacies [4,23]. However, these studies primarily focus on marine environments. In contrast, lacustrine fine-grained sedimentary rocks possess distinctive characteristics including limited geographic distribution, more intricate vertical stratigraphic relationships, diverse material composition, and a greater influence on depositional environments [24]. Therefore, the aforementioned research methodologies are not entirely applicable to the widely distributed lacustrine fine-grained sedimentary rocks in China.

The Dongying Sag is one of the key areas for the exploration of lacustrine fine-grained sedimentary rocks in China. The units from the upper fourth member (Es4u) to the lower third member (Es3l) of the Paleogene Shahejie Formation in this sag is characterized by rocks with stable thickness, moderate burial depth, high organic matter richness, and favorable types. Over 110 wells have discovered oil and gas in this area, indicating the potential for the generation and accumulation of tight oil and gas [25,26]. In recent years, Chinese scholars have conducted beneficial discussions and research on the lithofacies classification of fine-grained sedimentary rocks in the Dongying Sag and its surrounding areas. For instance, Liu et al. (2017) have focused on the division based on sedimentary structural and compositional characteristics, classifying the shale lithofacies of the Es3l to Es4u units of the Shahejie Formation in the Dongying Sag into three types such as laminated limestones and massive mudstones [27]. Liang et al. (2018), using organic matter content and mineral composition as main criteria, categorized the lacustrine shales of the Es4u interval of the Eocene Shahejie Formation in the Dongying Sag into eight lithofacies, including high-TOC calcareous shale and low-TOC calcareous shale [28]. Zhang et al. (2021), based on material composition, sedimentary structures, and genesis mechanisms, differentiated the fine-grained sedimentary rock lithofacies of the lower sub-member of the third member of the Paleogene Shahejie Formation in the Zhanhua Sag of the Bohai Bay Basin into five types, such as algal limestone and laminated recrystallized limestone [29]. Meanwhile, Liu et al. (2018) proposed classifying the fine-grained sedimentary rock lithofacies of the Es3l to Es4u units of the Eocene Shahejie Formation in the Jiyang Depression of the Bohai Bay Basin into lithofacies like thin lenticle crystalline limestone lithofacies and black shale lithofacies, based on rock type, macroscopic lamination characteristics, color, and other factors [30]. Previous studies show that the proposed classification methods vary depending on the used criteria and indicators, leading to significant differences. Furthermore, existing lithofacies classification schemes still fail to accurately reflect the petrological characteristics of fine-grained sedimentary rocks, lacking targeted, systematic, and practical lithofacies classification schemes.

Previous studies on the sedimentary environment and its evolution in the Dongying Sag have primarily focused on geochemical perspectives [31,32]. However, lithofacies and sedimentary environments are closely related. It is generally believed that organic-rich fine-grained sediments predominantly develop in deep-water environments during marine (or lacustrine) transgressive periods, usually found in stable marine (or lacustrine) basins, enclosed anoxic water bodies, and areas with low sedimentation rates. These conditions constitute the typical depositional model for organic-rich fine-grained sedimentary rocks. Nevertheless, recent field geological surveys and extensive experimental research show that organic-rich fine-grained sedimentary rocks can also form under relatively shallow water conditions. As research continues to deepen and experimental techniques advance, it has been found that the sedimentation process of fine-grained sedimentary rocks is often not stable. Factors like climate, provenance, and the physicochemical conditions of the water column all influence the process of fine-grained sedimentation and the development of organic-rich fine-grained sedimentary rocks [33]. Given the diverse lithologies and rapid vertical changes observed in the Dongying Sag's Es3l to Es4u units, a comprehensive analysis incorporating both lithofacies and geochemical methods is imperative for understanding the sedimentary evolution of the lake basin. Currently, such research, especially for the Es3l to Es4u interval in the Dongying Sag, is scarce, and the relationship between lacustrine fine-grained sedimentary rock lithofacies and controlling factor indicators remains unclear. Therefore, it is of paramount importance to analyze the alterations in sedimentary environmental characteristics and conduct comprehensive investigations into the genesis of fine-grained sedimentary rock lithofacies, as well as elucidate the intricate relationship between sedimentary environment evolution and lithofacies development, for the purpose of facilitating unconventional oil and gas exploration in the study area.

Building upon previous research, this study takes the Es3l–Es4u in Well Fanye1 of the Dongying Sag in the Bohai Bay Basin as an example and establishes the rock types and lithofacies ternary classification based on the observations in cores and thin sections, X-ray diffraction (XRD) tests, and geochemistry analysis. The coupling relationship between sedimentary environments and lithofacies is obtained by thoroughly analyzing the sedimentary environmental characteristics and the vertical evolution of lithofacies. This study contributes to a more comprehensive understanding of the characteristics of fine-grained sedimentary rocks, for the further prediction of the distribution of fine-grained sedimentary rock lithofacies from a sedimentary environment perspective, thereby providing geological insights to guide the exploration of lacustrine shale oil resources in China.

2. Geological Background

The Bohai Bay Basin, situated along the eastern coast of China, is a Cenozoic rift basin covering an area of about 200,000 square kilometers (Figure 1a). It is considered one of the richest oil and gas-bearing basins in China. The basin is subdivided into seven sub-basins: Linqing, Jizhong, Jiyang, Huanghua, Bozhong, Liaodong Bay, and Liaohe (Figure 1b) [34,35]. The formation of the Bohai Bay Basin is governed by the tectonic evolution of East Asia. During the Late Cretaceous to Paleogene, the Pacific Plate was subducted westward beneath the Eurasian Plate [36]. Around 55 Ma ago, the motion of the Pacific Plate slowed down, and its relative subduction beneath the Asian eastern margin receded, leading to the formation of a series of sedimentary basins, such as the Bohai Bay Basin [37].

The Dongying Sag, located in the southeastern part of the Jiyang Depression of the Bohai Bay Basin, is bordered by the Qingtuozi uplift to the east, the Binxian–Qingcheng uplift to the west, the Luxi uplift and the Guangrao uplift to the south, and the Chenjiazhuang uplift to the north (Figure 1c). It is a typical half-graben lake basin in China [38]. Previous studies indicate that the tectonic evolution of the Dongying Sag includes a Paleogene rifting stage (approximately 65 to 24.6 million years ago) and a post-rifting thermal subsidence stage (24.6 million years ago to the present). Based on sedimentation rates, the rifting stage is further subdivided into four phases (Rifting I–IV): the initial period (I), development

period (II), peak period (III), and atrophy period (IV) [39]. The Paleogene strata of the Dongying Sag comprise the Kongdian Formation, Shahejie Formation, and Dongying Formation from bottom to top (Figure 1d). The Shahejie Formation can be further divided into four sections, among which the fourth member can be subdivided into upper (Es4u) and lower sub-members (Es4l), the third section into upper (Es3u), middle (Es3m), and lower sub-members (Es3l), and the second section into upper (Es2u) and lower sub-members (Es2l) (Figure 1d) [39].

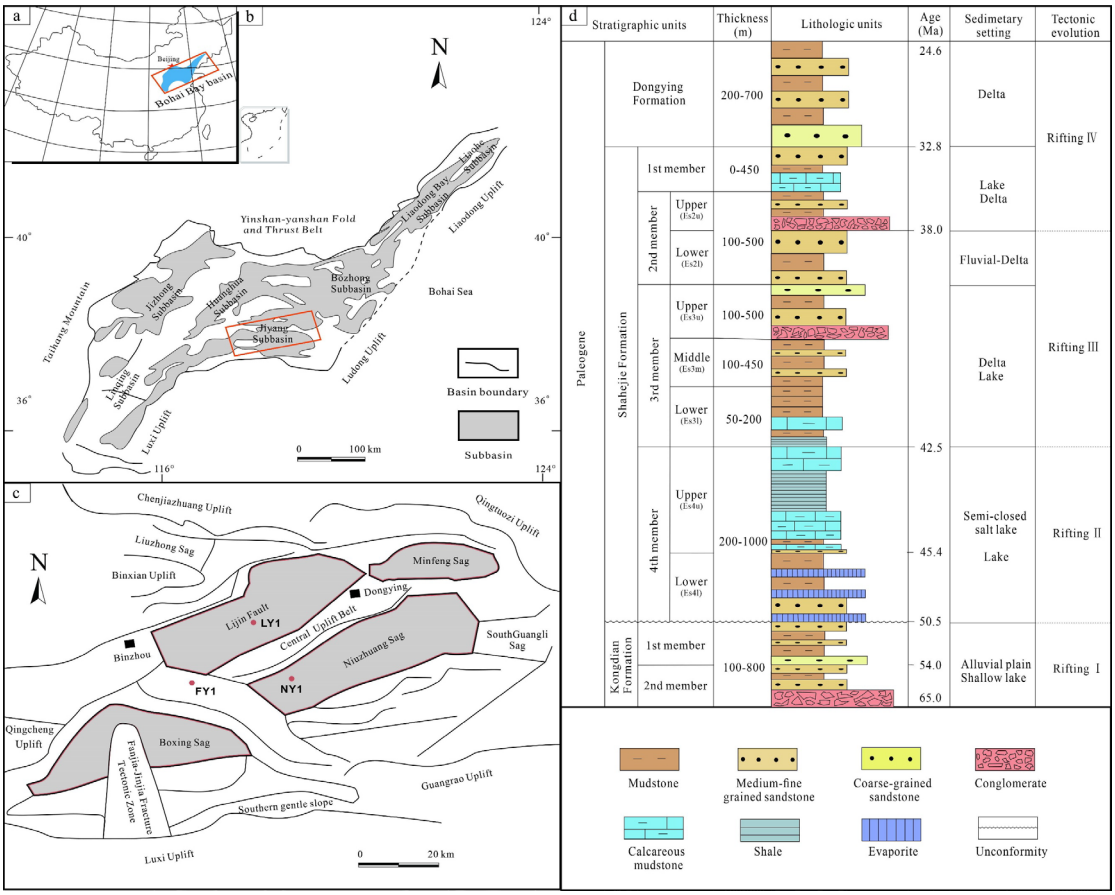

Figure 1. (**a**) Location of Bohai Bay Basin, (**b**) structural map of Bohai Bay Basin and location of Jiyang sub-basin, and (**c**) structural map of key well locations. (**d**) Sedimentary facies and stratigraphic column of the Dongying Sag.

The study interval spans from the Es4u to the Es3l of the Shahejie Formation. Es4u is primarily characterized by the development of carbonate rocks and shales, while Es3l is dominated by mudstones, both representing fine-grained sedimentary rocks (Figure 1d). These formations developed during the Rifting II to III periods, a time of the intense faulting and significant subsidence of the lake basin, leading to its large-scale expansion, with the lake area and water depth reaching their maximums [40]. Overall, the climate shifted from arid to humid conditions, gradually deepening the lake waters and resulting in the extensive development of semi-deep to deep lake facies; shallow lake facies are only found in the lower part of the Es4u interval [41]. Previous research has established the study interval as predominantly a semi-closed salt lake environment with anoxic bottom waters [42]. During this time, the prevailing warm and humid climate fostered an abundance of aquatic life, culminating in the accumulation of a significant quantity of organic matter. Consequently, this led to the formation of approximately 400 m of organic-rich fine-grained sedimentary rocks, suggestive of a high potential for hydrocarbon generation [43,44].

3. Methods

The samples for this study were obtained from Well Fanye1 in the Dongying Sag, with specific sampling depths ranging from 3030.23 m to 3443.90 m, encompassing the entire stratigraphic sequence from Es4u to Es3l. The sampling interval was set between 2 and 10 m, resulting in a total of 70 rock samples collected. All samples were cleaned, dried, and finely screened in the laboratory to ensure their representativeness and integrity.

Thin section examinations were conducted using a Leica DM4 polarizing microscope (Leica Microsystems Inc., Wetzlar, Germany), combined with our detailed description of approximately 414 m of core from Well Fanye1 in the study area. Systematic studies were conducted on the color, sedimentary structures, and mineral composition of fine-grained sedimentary rocks. XRD tests were performed using a D8 DISCOVER X-ray diffractometer (Bruker AXS GmbH, Kaunas, Lithuania), following the Chinese Oil and Gas Industry Standard SY/T 5163-2018 [45]. This analysis aimed to determine the overall mineral composition of the rock samples, with results expressed in percentages. All XRD analyses were completed at Petroleum Geology Research Center of the Shengli Oil field, Dongying, China.

The determination of the TOC was conducted at Petroleum Geology Research Center of the Shengli Oil field, using a LECO CS-600 carbon/sulfur analyzer (LECO Corporation, San Joseph, MI, USA), adhering to the Chinese National Standard GB/T 19145-2022 [46]. The measurements of major and trace elements were carried out at the Analysis and Testing Research Center of the Beijing Research Institute of Uranium Geology, Beijing, China. The concentrations of major elements were determined by a BrukerS1 TURBOSD portable X-ray fluorescence spectrometer (Bruker Corporation, Massachusetts, USA), with an analysis error controlled within 5%. Trace elements were measured using High resolution inductively coupled plasma mass spectrometer (Thermo Fisher Scientific, Bremen, Germany) by the Chinese National Standard GB/T 14506.30-2010 [47], ensuring the accuracy and reliability of the test results.

4. Results

4.1. Mineralogical Characterization

Mineral composition is the fundamental factor contributing to the diversity of lithofacies types in fine-grained sedimentary rocks and is the primary criterion for lithofacies classification. In the study area, the main mineral components of fine-grained sedimentary rocks include quartz, plagioclase, clay minerals, calcite, dolomite, and a minor amount of pyrite (Table 1). Overall, carbonate minerals (including calcite and dolomite) have the highest average content, approximately 49% (Table 1). However, the relatively large standard deviation indicates a wide range of variation in their content across different rocks. Calcite is the predominant carbonate mineral, showing little variation in the Es3l and Es4u units, with an average of 38.96% (Table 1); dolomite is almost exclusively found in Es4u, typically in isolated silt to fine sand-sized crystals, with an average content of 10.13% (Table 1). The average content of felsic minerals (mainly quartz and plagioclase) is 28.17% (Table 1), with quartz being the major component, averaging 24.09% (Table 1). Plagioclase follows, with a content of 4.08% (Table 1). The content of potassium feldspar is very limited and hence not included in the table. The content of clay minerals is relatively higher in Es3l (average 25.28%) and lower in Es4u (average 16.47%), with an overall average of 20.88% (Table 1). The variability in clay mineral content is lower than that of carbonate minerals but higher than that of felsic minerals. Pyrite, generally present in the form of framboidal pyrite, is relatively uniformly distributed across the entire interval, with an average content of about 2.67%.

Table 1. The total organic carbon content and whole-rock mineralogical composition of Es3l–Es4u fine-grained sedimentary rocks in the Dongying Sag.

Stratigraphic Units	TOC (%)	The Proportion of Mineral Composition (%)					
		Quartz	Plagioclase	Calcite	Dolomite	Pyrite	Clay
Es3l	1.18~4.20	10.00~37.00	1.00~19.00	12.00~60.00	0.00~13.00	0.00~11.00	8.00~41.00
	2.71 ± 1.30	23.66 ± 5.66	3.21 ± 2.11	37.12 ± 13.01	6.73 ± 6.76	2.82 ± 1.71	25.28 ± 9.40
Es4u	0.54~3.34	2.00~47.00	1.00~18.00	3.00~78.00	1.00~23.00	0.00~5.00	3.00~53.00
	2.14 ± 0.94	24.52 ± 8.94	4.95 ± 6.10	40.81 ± 20.28	13.53 ± 17.75	2.52 ± 3.05	16.47 ± 10.89
Total	0.54~4.20	2.00~47.00	1.00~19.00	3.00~78.00	0.00~23.00	0.00~11.00	3.00~53.00
	2.43 ± 1.18	24.09 ± 7.42	4.08 ± 4.54	38.96 ± 16.86	10.13 ± 13.61	2.67 ± 2.44	20.88 ± 11.05
Annotation:	1.18~4.20 / 2.71~1.30	=	Minimum value~Maximum value / Average ± Standard Deviation				

4.2. Geochemistry Characterization

The experimental results show that the organic matter contents are relatively high, ranging from 0.54% to 4.2%, with an average of 2.43%. However, there is a notable vertical variation. From the Es4u interval (0.54% to 3.34%, avg. 2.14%) to the Es3l interval (1.18% to 4.20%, avg. 2.71%), there is an upward trend in organic matter content (Table 1). Specifically, there are more rocks with less than 2% organic matter content in the Es4u interval, whereas the proportion of rocks with more than 2% organic matter is higher in the Es3l interval (Figure 2).

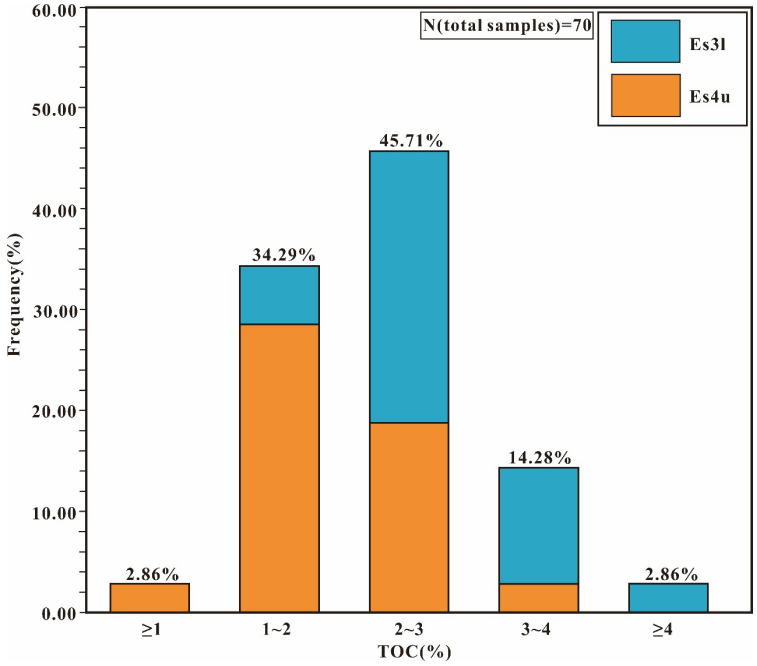

Figure 2. Frequency distribution of TOC (%) in Es3l–Es4u of Shahejie Formation of Dongying Sag, Bohai Bay Basin.

The major elements include Al (1.21% to 11.31%, avg. 4.23%), Ca (2.65% to 29.09%, avg. 17.39%), K (0.24% to 2.44%, avg. 0.94%), Na (0.13% to 2.54%, avg. 0.42%), P (0.03% to 0.20%, avg. 0.085%), and Ti (0.07% to 0.77%, avg. 0.25%). The trace elements include Ba (236 μg to 5558 μg, avg. 631.33 μg), Sr (481 μg to 9755 μg, avg. 2346.81 μg), V (26.3 μg to 165 μg, avg. 70.7 μg), Sc (2.67 μg to 31.3 μg, avg. 9.85 μg), and Ni (16.1 μg to 58.4 μg, avg.

34.3 μg). In all shale samples, some major elements show significant vertical fluctuations in relative concentrations, while trace elements exhibit less obvious vertical fluctuations (Figure 3).

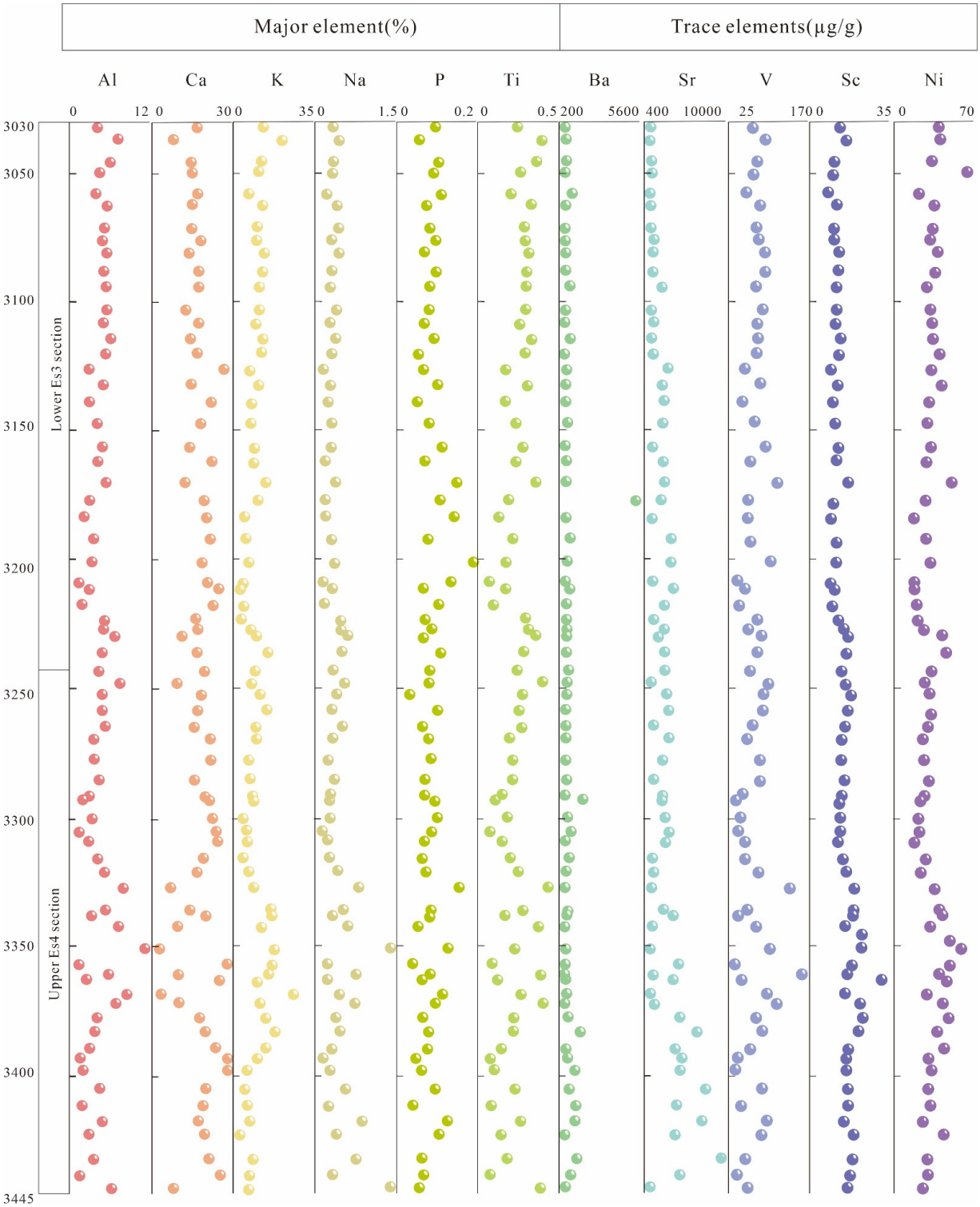

Figure 3. The distribution of major and trace elements in the Es3l–Es4u fine-grained sedimentary rocks of the Dongying Sag.

4.3. Rock Type Classification

Based on previous research results and petrological observations, the lithologies of the study interval include siltstone, mudstone, and carbonate rocks, representing fine-grained sedimentation [48]. Considering the background of the study area and the results of XRD, this study proposes a ternary lithology classification system and divides the rocks into three categories: carbonate minerals, felsic minerals, and clay minerals. Using a threshold of 50% content for each category, fine-grained sedimentary rocks are initially classified into four major types: fine-grained felsic sedimentary rocks (I), clay rocks (II), carbonate rocks (III), and fine-grained mixed sedimentary rocks (IV, V, VI) (Figure 4).

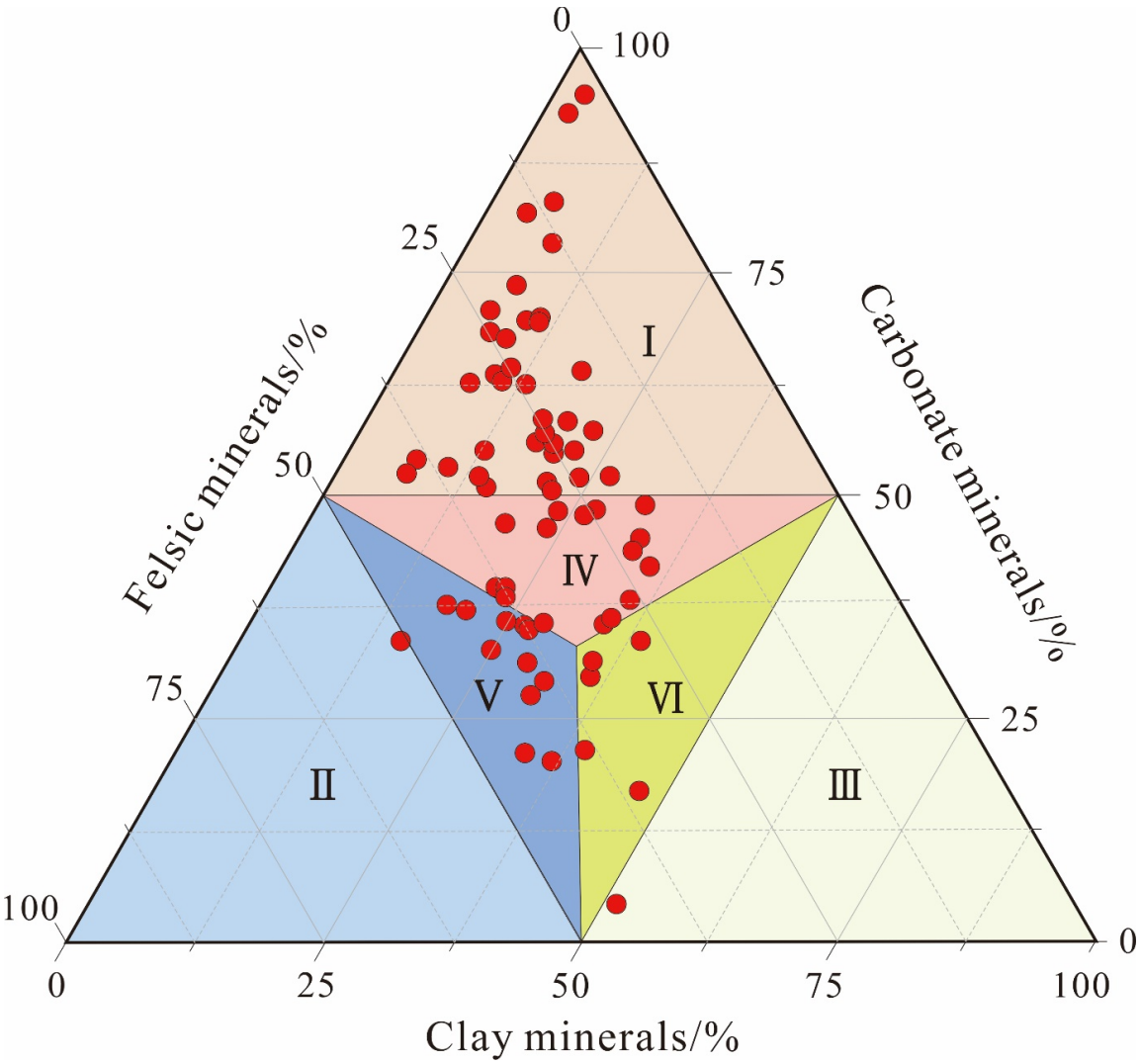

Figure 4. Ternary diagram of main mineral content of fine-grained sedimentary rocks in Dongying Sag and lithology classification. (I) Carbonate rock, (II) fine-grained felsic sedimentary rock, (III) clay rocks, (IV) carbonate fine-grained mixed sedimentary rock, (V) felsic fine-grained mixed sedimentary rock, (VI) clayey fine-grained mixed sedimentary rock.

For fine-grained felsic sedimentary rocks, clay rocks, and carbonate rocks, the principal mineral component exceeding 50% content is used as the basic name of the rock. It is important to note that in carbonate rocks, the principal name, limestone or dolomite, is determined based on whether calcite or dolomite has a higher relative content. For a rock with a mineral component content between 25% and 50%, this component is prefixed to the basic name. For example, a fine-grained sedimentary rock with 60% carbonate (more calcite than dolomite), 30% felsic, and 10% clay content is named felsic limestone. In the category

of fine-grained mixed sedimentary rocks, where no mineral component exceeds 50%, the rock is named based on the highest content among the three categories of carbonate, felsic, and clay minerals. For instance, a rock with 45% carbonate, 35% felsic, and 20% clay content is named carbonate fine-grained mixed sedimentary rock. Following this classification scheme, the rocks in the study area are primarily categorized as Class I carbonate rocks and Class IV carbonate fine-grained mixed sedimentary rocks, followed by Class V felsic fine-grained mixed sedimentary rocks and Class VI clayey fine-grained mixed sedimentary rocks, with Class II fine-grained felsic sedimentary rocks and Class III clay rocks being the least developed.

4.4. Lithofacies Classification Scheme and Main Lithofacies Types

Building on our rock classification, we divided the lithofacies according to three principles: (1) clear boundaries and definitive meanings, (2) distinct distinguishing characteristics between categories, and (3) relevance to the analysis of genetic mechanisms [49]. Thus, we employed "mineral composition + sedimentary structure + organic matter content" for the classification and naming of lithofacies. Mineral composition, as the fundamental factor in rock type diversity and the result of both sedimentary and post-sedimentary processes, forms the material basis. Sedimentary structures reflect sediment input and hydrodynamic conditions. The organic matter component, which is widely distributed in the rocks of the study area, exerts a significant influence on diagenesis and the oil-bearing properties of fine-grained sedimentary rocks integrated with source–reservoir, thus necessitating its incorporation into lithofacies nomenclature. Lithofacies with more than 2% organic matter are classified as organic-rich lithofacies, accounting for about 62.85% (Figure 5a); those with 1% to 2% organic matter are organic-moderate lithofacies, representing 34.29% (Figure 5a); and those with less than 1% organic matter are organic-poor lithofacies, the least common at 2.86% (Figure 5a). Regarding sedimentary structures, those with single-layer thicknesses less than 1 mm are classified as laminated, more than 1 mm as layered, and those with unclear bedding structures as massive [50]. In the study interval from Es3l to Es4u, developed laminated structures make up 80%, layered structures are extremely rare at 1.43%, and massive structures account for 18.57% (Figure 5b).

According to this classification scheme, the Es3l to Es4u units developed 18 lithofacies (Table 2), with seven main lithofacies constituting 62.86% of the total. These are organic-rich laminated limestone lithofacies (ORLL), organic-moderate massive limestone lithofacies (OMML), organic-moderate laminated felsic limestone lithofacies (OMLFL), organic-rich laminated carbonate fine-grained mixed sedimentary rock lithofacies (ORLCMR-1), organic-rich laminated felsic fine-grained mixed sedimentary rock lithofacies (ORLFMR), organic-rich laminated clayey fine-grained mixed sedimentary rock lithofacies (ORLCMR-2), and organic-rich massive carbonate fine-grained mixed sedimentary rock lithofacies (ORMCMR) (Figure 5c). Based on microscopic observations of thin sections combined with geochemical parameter characteristics, different primary lithofacies are described, and their developmental environments are discussed.

Table 2. Comprehensive classification and nomenclature scheme of Es3l–Es4u fine-grained sedimentary rock lithofacies in Dongying Sag.

Lithofacies	Lithofacies Association	Clay/%	Felsic/%	Carbonates/%	Interrelation
Carbonate lithofacies	ORLL, OMLL	0~25	0~25	50~100	Vca > Vfe; Vca > Vcl
	ORML, OMML, OPML	0~25	0~25	50~100	Vca > Vfe; Vca > Vcl
	ORLFL, OMLFL	0~25	25~50	50~100	Vca > Vfe > Vcl
	ORMCL	25~50	0~25	50~100	Vca > Vcl >Vfe
Claystone lithofacies	ORLFC	50~100	25~50	0~25	Vcl > Vfe > Vca
Fine-grained felsic sedimentary lithofacies	ORLLF	0~25	50~100	25~50	Vfe > Vca > Vcl

Table 2. *Cont.*

Lithofacies	Lithofacies Association	Clay/%	Felsic/%	Carbonates/%	Interrelation
Fine-grained mixed sedimentary lithofacies	ORLCMR-1, OMLCMR-1, OPLCMR-1	0~50	0~50	33.33~50	Vca > Vfe; Vca > Vcl
	ORLFMR, OMLFMR	0~50	33.33~50	0~50	Vfe > Vca; Vfe > Vcl
	ORLCMR-2	33.33~50	0~50	0~50	Vcl > Vfe; Vcl > Vca
	ORMCMR, OMMCMR	0~50	0~50	33.33~50	Vca > Vfe; Vca > Vcl

Annotation: Eighteen lithofacies of the Es3l to Es4u fine-grained sedimentary rocks: (1) organic-rich/moderate laminated limestone lithofacies (ORLL/OMLL), (2) organic-rich/moderate/poor massive limestone lithofacies (ORML/OMML/OPML), (3) organic-rich/moderate laminated felsic limestone lithofacies (ORLFL/OMLFL), (4) organic-rich massive clayey limestone lithofacies (ORMCL), (5) organic-rich laminated felsic clay rock lithofacies (ORLFC), (6) organic-rich layered limy fine-grained felsic sedimentary rock lithofacies (ORLLF), (7) organic-rich/moderate/poor laminated carbonate fine-grained mixed sedimentary rock lithofacies (ORLCMR-1/OMLCMR-1/OPLCMR-1), (8) organic-rich/moderate laminated felsic fine-grained mixed sedimentary rock lithofacies (ORLFMR/OMLFMR), (9) organic-rich laminated clayey fine-grained mixed sedimentary rock lithofacies (ORLCMR-2), (10) organic-rich/moderate massive carbonate fine-grained mixed sedimentary rock lithofacies (ORMCMR/OMMCMR), (11) Vca = carbonate mineral content; Vcl = clay mineral content; Vfe = felsic mineral content.

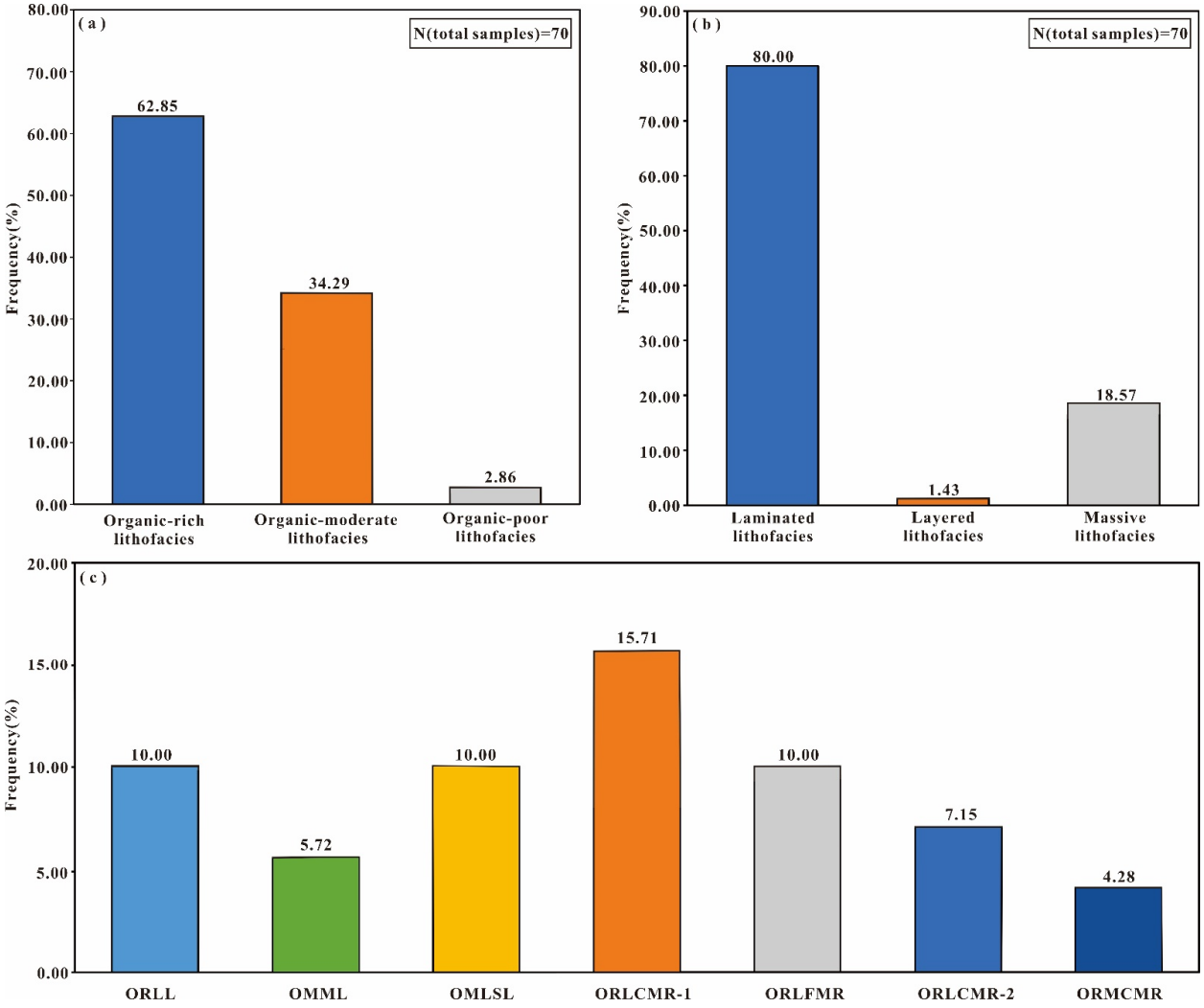

Figure 5. Bar graphs representing the characteristics of the Es3l–Es4u lithofacies in the Dongying Sag. (**a**) Fine-grained sedimentary rocks' classification based on TOC content, (**b**) fine-grained sedimentary rocks' classification based on sedimentary structure; (**c**) the frequency of major lithofacies from Es3l–Es4u fine-grained sedimentary rocks in Well Fanye1 in the Dongying Sag.

4.4.1. Organic-Rich Laminated Limestone Lithofacies

ORLL are widely distributed in the study interval, predominantly in Es4u. They are primarily composed of carbonate minerals (avg. 64.40%), followed by felsic minerals (avg. 19.50%), with the least content of clay minerals (avg. 13.50%). The TOC content ranges from 2.16% to 3.28%, averaging 2.63% (Table 3). The core generally appears gray-black with distinct light–dark boundaries (Figure 6a). Under microscopic observation, there are well-developed alternating light and dark thin laminated structures, with the light layers thicker than the dark ones. The laminae are continuous, often appearing wavy (Figure 7a) and sometimes discontinuous and lens-shaped (Figure 7b). The light layers primarily consist of carbonate minerals, while the dark layers are predominantly organic-rich clay. Fine quartz grains are observed semi-oriented between layers (Figure 7b). Calcite minerals in the samples appear predominantly as hidden crystals, with some recrystallized into coarse, clean, bright fibrous structures. These bright fibrous structures grow perpendicular to the laminae, exhibiting a distinct crystal form. Dark, organic-rich clay layers can be seen interbedded between lighter calcite layers (Figure 7c). This lithofacies in the lower section of Es4u often contains well-formed microcrystalline dolomite, distributed in isolated or clumped patterns, often rhombohedral (Figure 7d).

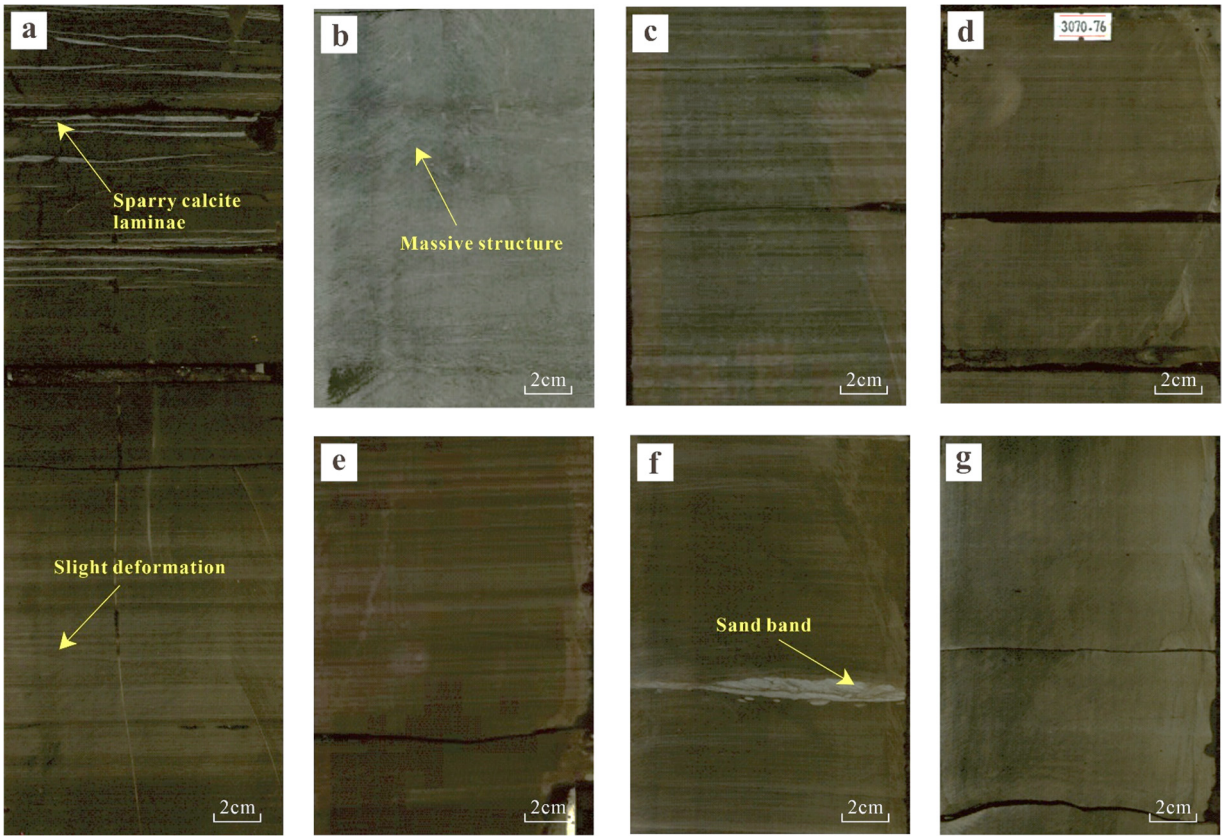

Figure 6. Macroscopic characteristics of seven commonly seen lithofacies in Es3l–Es4u. (**a**) Organic-rich laminated limestone lithofacies, Well Fanye1, 3248.47 m, (**b**) organic-moderate massive limestone lithofacies, Well Fanye1, 3390.54 m, (**c**) organic-moderate laminated felsic limestone lithofacies, Well Fanye1, 3337.20 m, (**d**) organic-rich laminated carbonate fine-grained mixed sedimentary rock lithofacies, Well Fanye1, 3070.76 m, (**e**) organic-rich laminated felsic fine-grained mixed sedimentary rock lithofacies, Well Fanye1, 3155.26 m, (**f**) organic-rich laminated clayey fine-grained mixed sedimentary rock lithofacies, Well Fanye1, 3102.40 m, (**g**) organic-rich massive carbonate fine-grained mixed sedimentary rock lithofacies, Well Fanye1, 3057.80 m.

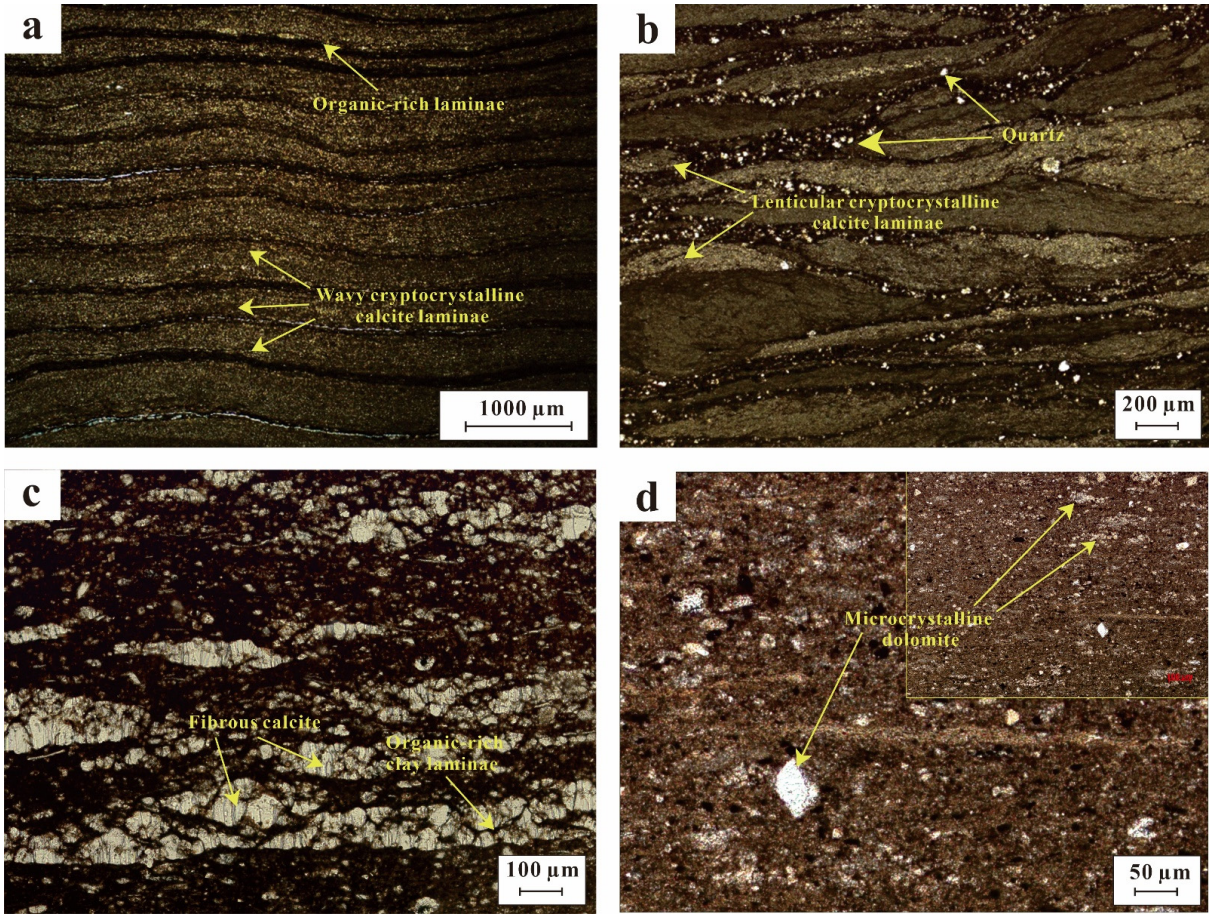

Figure 7. Microscopic characteristics of ORLL. (**a**) Wavy cryptocrystalline calcite laminae, Well Fanye1, 3200.15 m, (**b**) lenticular cryptocrystalline calcite laminae, Well Fanye1, 3208.03 m, (**c**) bright fibrous structures of recrystallized calcite, Well Fanye1, 3388.19 m, (**d**) well-formed microcrystalline dolomite, Well Fanye1, 3396.54 m.

Table 3. The average value of the mineral composition and TOC of different main lithofacies.

Lithofacies Association	Clay Minerals (%)	Felsic Minerals (%)	Carbonate Minerals (%)	TOC (%)
ORLL	6~21	11~24	51~80	2.16~3.28
	13.50	19.50	64.40	2.63
OMML	3~22	2~24	54~95	1.18~1.83
	13.67	18.00	67.00	1.52
OMLFL	7~14	26~36	51~65	1.29~1.93
	10.00	29.63	58.88	1.61
ORLCMR-1	19~36	19~36	34~49	2.17~4.00
	27.29	25.12	42.47	2.79
ORLFMR	21~37	37~44	19~37	2.12~3.86
	25.82	41.36	28.18	3.02
ORLCMR-2	34~48	27~37	16~33	2.04~2.51
	39.56	31.67	23.67	2.28
ORMCMR	23~28	25~28	36~46	2.25~2.53
	25.00	26.33	43.67	2.41
Annotation:	6~21 / 13.50	=	Minimum value~Maximum value / Average	

4.4.2. Organic-Moderate Massive Limestone Lithofacies

OMML predominantly develops in the basal part of the Es4u interval. The primary mineral components are dominated by carbonate minerals (avg 67.00%), followed by felsic minerals (avg 18.00%), with a relatively lower content of clay minerals (avg 13.67%). The TOC content ranges between 1.18% and 1.83%, averaging 1.52% (Table 3). Due to the low organic content, the core color is lighter, appearing gray-white, with a massive structure (Figure 6b). The carbonate minerals are almost entirely cryptocrystalline calcite, mixed with clay minerals. Felsic minerals are sparsely distributed, with occasional bioclasts and pyrite visible (Figure 8a).

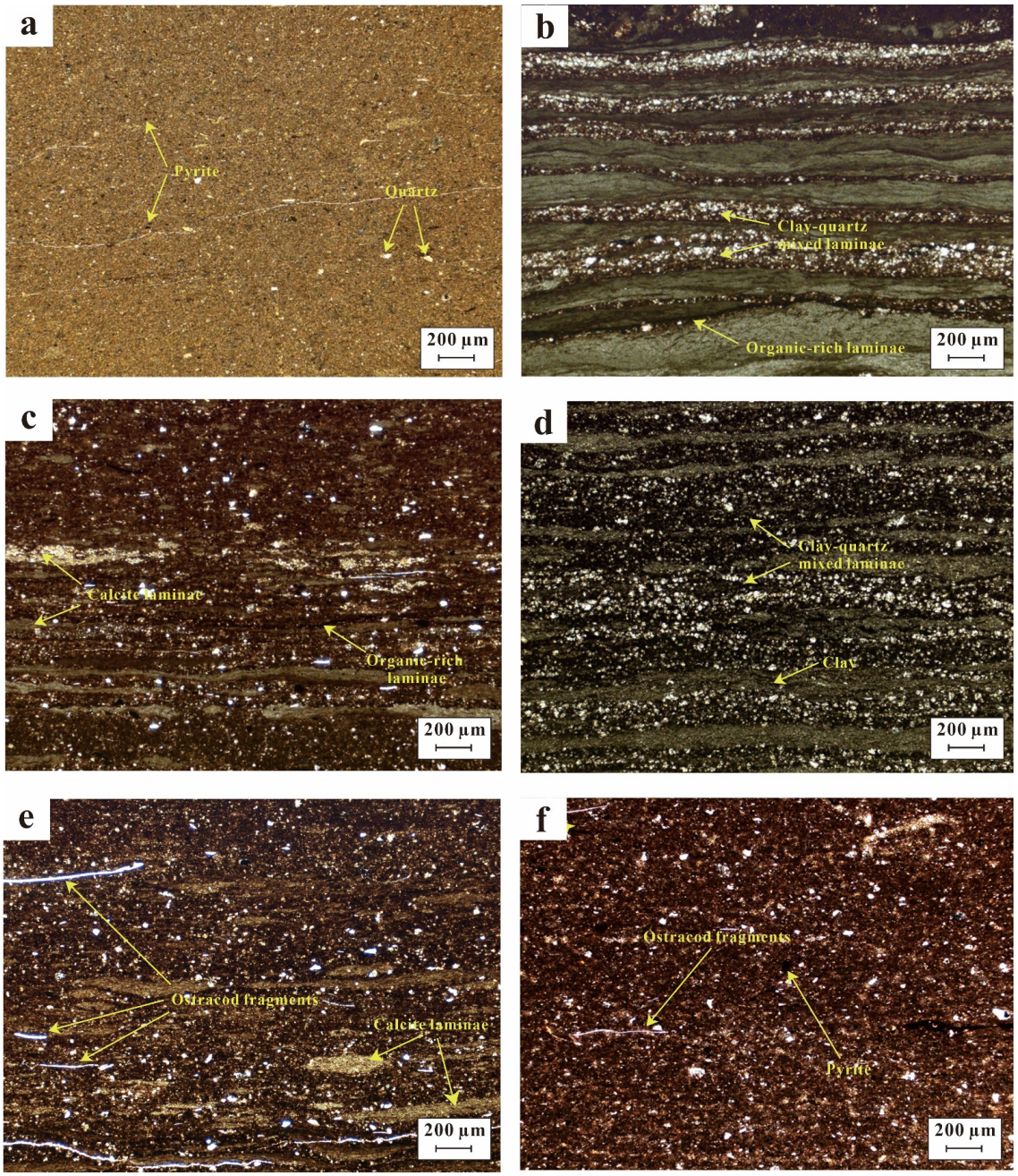

Figure 8. Microscopic characteristics of the other six commonly seen lithofacies in Es3l–Es4u. (**a**) OMML, Well Fanye1, 3235.01 m, (**b**) OMLFL, Well Fanye1, 3361.84 m, (**c**) ORLCMR-1, Well Fanye1, 3140.38 m, (**d**) ORLFMR, Well Fanye1, 3376.84 m, (**e**) ORLCMR-2, Well Fanye1, 3191.21 m, (**f**) ORMCMR, Well Fanye1, 3059.23 m.

4.4.3. Organic-Moderate Laminated Felsic Limestone Lithofacies

OMLFL is primarily distributed in the upper part of the Es4u interval and the lower part of the Es3l interval. Compared to limestone, OMLFL has a higher content of felsic minerals (avg 29.63%), followed by carbonate minerals (avg 58.88%), and the least amount of clay minerals (avg 10.00%) (Table 3). The TOC ranges from 1.29% to 1.93%, averaging 1.61% (Table 3). The core primarily appears gray, exhibiting a structure with alternating light and dark laminations (Figure 6c). Under microscopic observation, light cryptocrystalline calcite laminae exhibit laterally discontinuous extensions with undulating waves in the laminated structures and distinct contact boundaries between laminae. The dark laminae are mainly composed of a mixture of felsic and clay minerals, with occasional individual organic thin layers (Figure 8b).

4.4.4. Organic-Rich Laminated Carbonate Fine-Grained Mixed Sedimentary Rock Lithofacies

ORLCMR-1 is predominantly found in the middle part of the Es3l interval and rarely seen in the Es4u interval, and it is the most extensively developed lithofacies type in the study interval. From a mineralogical perspective, the content of each mineral type is less than 50% (Table 3). Carbonate minerals have the highest content (avg 42.47%), closely followed by clay minerals (avg 27.29%) and felsic minerals (avg 25.12%). The TOC content ranges from 2.17% to 4.00%, averaging 2.79% (Table 3). Overall, the core appears gray-black (Figure 6d). Under microscopic observation, similar to ORLL, the light laminae are primarily cryptocrystalline or microcrystalline calcite lamina, composed of discontinuous gray mud lenses. The dark layers mainly consist of clay–quartz mixture laminae with higher organic content. Notably, the thickness of the light-colored layers is significantly less than that of the dark layers. There is no dominant mineral component, with organic matter dispersedly enriched in the clay laminae (Figure 8c).

4.4.5. Organic-Rich Laminated Felsic Fine-Grained Mixed Sedimentary Rock Lithofacies

ORLFMR is primarily distributed in the middle to lower part of the Es3l interval, with a few occurrences in the Es4u interval. In terms of mineral composition, it is dominated by felsic minerals (avg 41.36%), followed by clay minerals (avg 25.82%) and carbonate minerals (avg 28.18%) (Table 3). The TOC content ranges from 2.12% to 3.86%, averaging 3.02% (Table 3). The core is composed of frequent vertical intercalations of light and dark lamina (Figure 6e). The light layers mainly consist of cryptocrystalline calcite, quartz, and feldspar, with a small amount of clay minerals filling the pores. The dark layers are composed of quartz and organic-rich clay minerals. The laminae exhibit wavy undulations (Figure 8d).

4.4.6. Organic-Rich Laminated Clayey Fine-Grained Mixed Sedimentary Rock Lithofacies

ORLCMR-2 is primarily found in the middle and top sections of the Es3l interval. It has a high content of clay minerals (avg 39.56%), a moderate amount of felsic minerals (avg 31.67%), and a relatively lower proportion of carbonate minerals (avg 23.67%) (Table 3). The TOC ranges from 2.04% to 2.51%, averaging 2.28% (Table 3). The core appears dark gray, occasionally interspersed with sandy bands (Figure 6f). Some samples of this lithofacies contain indistinctly bordered lens-shaped laminations and a few with well-developed, clearly bordered thin lamina. Since the light layers consist of both cryptocrystalline calcite and clay minerals, the contrast between light and dark lamina is not distinct. The dark laminae are mainly a mixture of clay minerals, felsic minerals, organic matter, and pyrite. Common occurrences of ostracod and algal fragments are observed, oriented along the layers.

4.4.7. Organic-Rich Massive Carbonate Fine-Grained Mixed Sedimentary Rock Lithofacies

ORMCMR is primarily developed in the Es3l interval; this lithofacies has mineral content characteristics similar to those of ORLCMR-1 (Table 3). The TOC content ranges from

2.25% to 2.53%, averaging 2.41% (Table 3), and the core lacks distinct layering (Figure 6g). Under microscopic observation, felsic minerals, clay minerals, and cryptocrystalline carbonate minerals are uniformly mixed. Locally, pyrite and ostracod fragments can be seen; sporadically, minor cryptocrystalline to microcrystalline calcite lenses form discontinuous laminae. The poor sorting and rounding of the felsic minerals indicate that this lithofacies is a product of turbidite sedimentation. Pyrite exists in the form of framboidal pyrite, and the clay minerals, due to adsorbing a significant amount of organic matter, partly exhibit a darker color (Figure 8f).

4.5. Paleoenvironment Reconstruction

The distribution of elements within rock strata is influenced not only by the physical and chemical properties of the elements themselves but also by the sedimentary environment [51]. Therefore, we utilize a variety of inorganic geochemical parameters to interpret the sedimentary environment. These proxies include paleoclimate proxies (CIA, Na/Al), paleoproductivity proxies (Ba), paleosalinity proxies (Sr/Ba), paleo-redox proxies (V/Sc, V/V + Ni), and terrigenous detrital input proxies (Al, Ti). Through the analysis of these parameters, the overall environmental characteristics during the shale sedimentation period of the Es3l–Es4u units are analyzed (Figure 9).

4.5.1. Paleoclimate Conditions

Paleoclimate can broadly influence sedimentary environments, including direct impacts on the paleosalinity of water bodies, marine (or lacustrine) currents, and the influx of terrigenous material. Moreover, it can indirectly influence the redox conditions of water bodies and control water stratification, among other effects [52]. We study the paleoclimatic characteristics of the period of deposition using geochemical data such as the CIA and Na/Al ratios.

The CIA reflects the degree of chemical weathering experienced by rocks, as indicated by the ratio of enriched alkali metals (e.g., aluminum, sodium, and potassium) to alkaline earth metals (such as calcium). It is widely employed for analyzing variations in paleoclimate [53]. The index is calculated as CIA = moles $[(AlO_3)/(Al_2O_3 + CaO^* + Na_2O + K_2O)] \times 100$, where $CaO^* = CaO\text{-}(10 \times P_2O_5/3)$. If the corrected mole number of CaO is less than that of NaO, then the corrected CaO mole number is used; otherwise, the Na_2O mole number is used [54]. High CIA values (85~100) in sediments indicate intense humid and hot climatic conditions; medium values (70~85) suggest warm and moist climatic conditions, while lower values (50~70) represent cold and dry climatic conditions [55]. In general, the CIA values exhibit an increasing trend (from 54.03 to 79.60, avg. 72.24) (Figure 9), suggesting a gradual transition from cold and arid to warm and moist conditions in the Es3l to Es4u paleoclimate, resulting in the heightened chemical weathering of rocks. However, the CIA cannot be the sole proxy of climatic change due to its susceptibility to various other factors, such as sediment provenance and depositional conditions [55]. Hence, it is necessary to perform a comprehensive analysis combining other geological and climatic proxies. The Na/Al ratio also effectively reflects the climatic conditions during sediment deposition [3], with higher ratios typically indicating arid climates and vice versa [26,56]. The Na/Al ratios show a gradual decrease from the bottom to the top (Figure 9). Two proxies suggest that the paleoclimate during the Es3l–Es4u depositional period gradually became warmer and moister, consistent with previous research findings [26,57].

4.5.2. Paleoproductivity

Paleoproductivity refers to the organic productivity level of an ecosystem in a specific area or period in Earth's history. By monitoring changes in paleoproductivity, we can obtain crucial information about the paleoclimate, water salinity, nutrient supply, and ecological interactions in the study area. Contemporary oceanographic research has established barium (Ba) as one of the widely used proxies of paleoproductivity [58]. Numerous studies indicate that phytoplankton can enrich Ba in water. Furthermore, during the decomposition

of these organisms, the high concentrations of sulfate (SO_4^{2-}) on their surfaces can react with Ba^{2+} ions to form barite ($BaSO_4$), which then precipitates and accumulates [59,60]. Therefore, Ba enrichment indicates high primary productivity in surface waters, and vice versa.

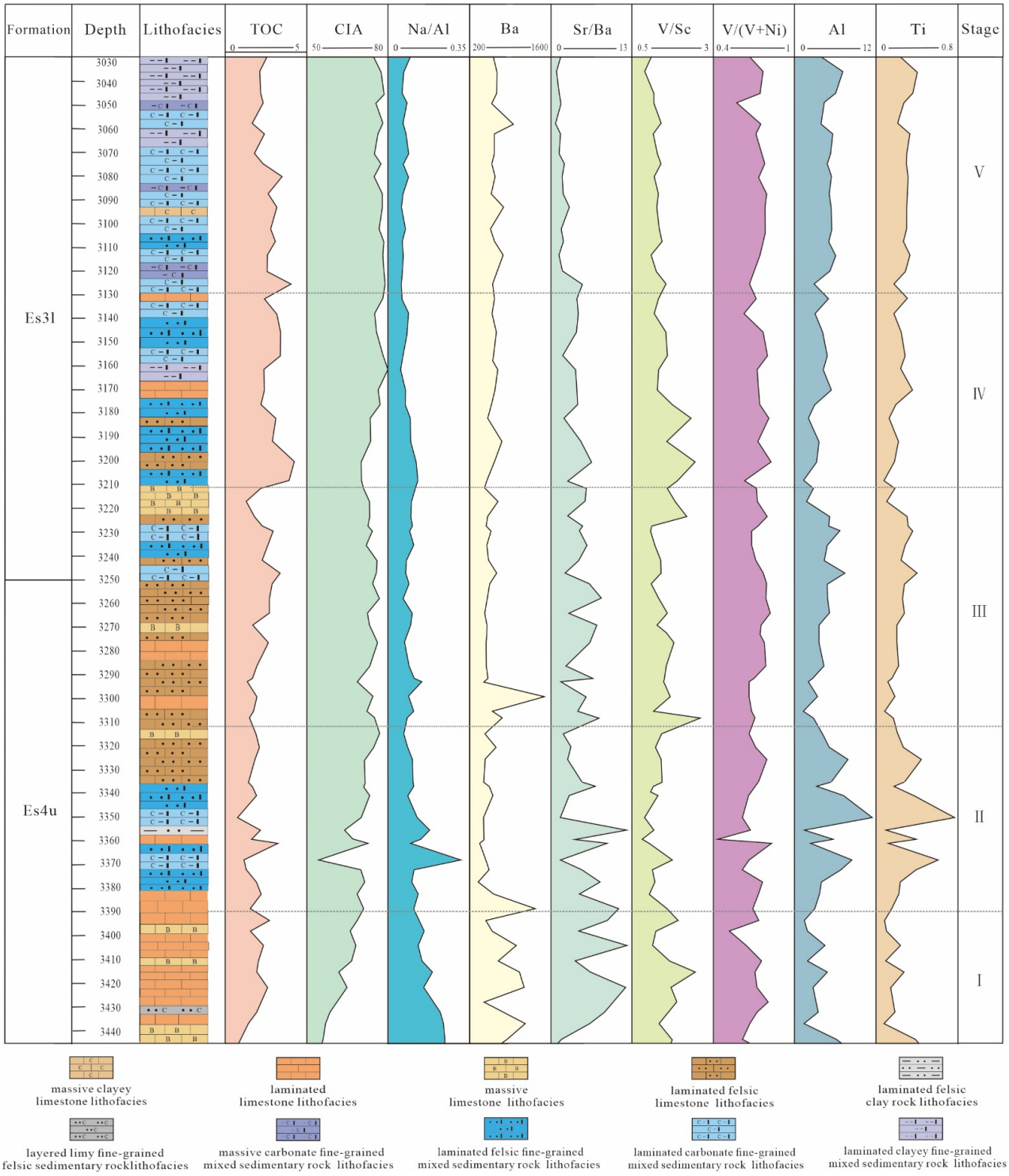

Figure 9. The stratigraphic variation in TOC, paleo-redox, paleosalinity, paleoclimate, paleoproductivity, and terrigenous detrital influx in the Es3l–Es4u of the Shahejie Formation of the Dongying Sag, Bohai Bay Basin.

In the Es3l–Es4u units, Ba content shows high values in the lower part of the Es4u interval (avg. 774.67 μg), then rapidly decreases near 3380 m, followed by a relatively steady upward trend (Figure 9). The target layers overall maintain a high level of productivity. The sudden decrease in productivity in the middle to lower part of the Es4u interval may be related to frequent storm events during that period (discussed in detail in Section 5.1.2).

4.5.3. Paleosalinity

Paleosalinity refers to the salinity of water bodies during sediment deposition and has a significant impact on the development of organic-rich fine-grained sedimentary rocks [61]. Typically, elevated salinity levels can induce water stratification, impeding convective mixing and hindering sediment–oxygen contact, thereby promoting the preservation of organic matter [62,63]. Sr/Ba ratios are commonly used to indicate changes in paleosalinity, with fine-grained sedimentary rocks having higher Sr/Ba values considered to have experienced high-salinity depositional environments [64]. When Sr/Ba exceeds 1.0, it indicates saline water conditions; values between 0.6 and 1.0 suggest brackish water; and values below 0.6 are indicative of freshwater [55,65]. Additionally, high Sr content also suggests arid conditions, consistent with the high salinity indicated by high Sr/Ba values.

In the Es3l–Es4u units, the average Sr/Ba content is (12.02~0.70, avg. 4.34) (Figure 9), reflecting an overall saline lake environment. The ratio gradually decreases from bottom to top, attributed to the progressive increase in humidity and precipitation, resulting in the dilution of lake water and subsequent salinity reduction. Furthermore, the high content of carbonate minerals (especially dolomite) in the Es4u interval (Table 1) reflects a high-salinity evaporative environment during that period [66].

4.5.4. Paleo-Redox

Redox conditions in lake waters are pivotal in sedimentary environment studies, directly influencing the diversity and quantity of aquatic lifeforms and the preservation of biological material post-mortem. These conditions also affect the migration and deposition of elements within the lake. When investigating trace elements sensitive to depositional environment redox states, their enrichment levels can reflect the redox conditions of the water during sedimentation [67].

V tends to be enriched in reducing environments, while nickel accumulates more readily in oxidizing conditions. Thus, the ratio of V/V + Ni in sediments can be utilized to infer the paleo-redox conditions of the water column [68]. For instance, a V/(V + Ni) ratio greater than 0.6 indicates reducing conditions in the water body [69], with most V/(V + Ni) ratios exceeding the threshold (0.44–0.79, avg. 0.67) (Figure 9). This suggests that the fine-grained sedimentary rocks from the Es3l to Es4u units predominantly formed in reducing depositional environments. The V/Sc ratio is also widely acknowledged as an effective proxy of paleo-redox conditions [64]. A V/Sc ratio above 7.9 typically suggests anoxic conditions [70]. The average V/Sc value across the Es3l to Es4u units (3.76–16.29, avg. 7.89) indicates an environment ranging from oxygen-poor to reducing conditions (Figure 9). Additionally, pyrite often serves as an indicator of the paleo-redox conditions of water bodies, preserved when oxygen content is low or when oxygen is unable to reach certain areas. The XRD analyses indicate that pyrite is extensively distributed within Es3l–Es4u (Table 1). Integrating these geochemical proxies, the paleo-lake basin in the Es3l to Es4u units of the Dongying Sag was in a reducing environment.

It is noteworthy that in the middle part of Es4u, both geochemical proxies exhibit notable fluctuations towards weakly reducing conditions. It suggests that this period was possibly influenced by storms or similar events with the introduction of oxygen into the lake.

4.5.5. Terrigenous Detrital Influx

Aluminum (Al) and Titanium (Ti) are commonly utilized as proxies of terrigenous detrital input [71]. Al, a major constituent of continental crust rocks, soils, and their

weathering products, typically exists as part of minerals within the lattices of feldspars and clay minerals in the form of layered silicate minerals, exhibiting notable stability [72]. Al concentrations exhibit a distinct pattern within the Es4u interval, characterized by low values at the base, followed by a rapid increase in the middle section accompanied by significant fluctuations. Subsequently, there is a sharp decrease towards the upper part of Es4u, eventually stabilizing into a moderately increasing trend towards the top of Es3l (Figure 9). Excluding the oscillatory region in the mid-section of Es4u (3340 m–3380 m), the average Al content in Es4u (1.02%–0.06%, avg. 0.26%) is considerably lower than that in Es3l (1.02%–0.08%, avg. 0.32%), indicating a fluctuating increase in terrigenous detrital influx from Es4u to Es3l.

Ti, another major component of the continental crust, is typically found in lower concentrations in mafic-dominated oceanic crust and is frequently associated with high-energy terrigenous detrital and coarse-grained sedimentary environments [73,74]. It also serves as a proxy of terrigenous material. The trend of Ti content in Es4u (excluding the 3340 m–3380 m region) averages 0.44%–0.08%, avg. 0.21%, which is lower than in Es3l (0.40%–0.07%, avg. 0.26%). A significant positive correlation between the TiO_2 and Al_2O_3 content in the Es3l to Es4u interval (Figure 10), with a correlation coefficient R2 = 0.955, indicates a close association with terrigenous input, supporting the effectiveness of these proxies in assessing terrigenous detrital influx [50,64]. The sharp rise and subsequent decline in the Ti content in the middle of Es4u, combined with other geochemical proxies, suggest a gradual overall increase in terrigenous detrital influx from the bottom to the top of Es3l–Es4u. Considering that the lithofacies of Es3l are dominated by limestone facies, and Es4u is characterized by fine-grained mixed sedimentary rock lithofacies, the combined proportion of felsic minerals and clay minerals in Es3l is significantly higher than in Es4u. It is likely due to variations in terrigenous detrital supply, indicating an increasing trend of terrigenous detrital influx from the bottom to the top of the interval. This trend is likely controlled by paleoclimatic factors, with a moist climate potentially leading to greater terrigenous detrital influx. Similar to the redox proxies' trends, the terrigenous proxies in the middle part of Es4u also exhibit strong fluctuations, reflecting a period of substantial terrigenous detrital influx, which is likely related to storm events occurring at that time.

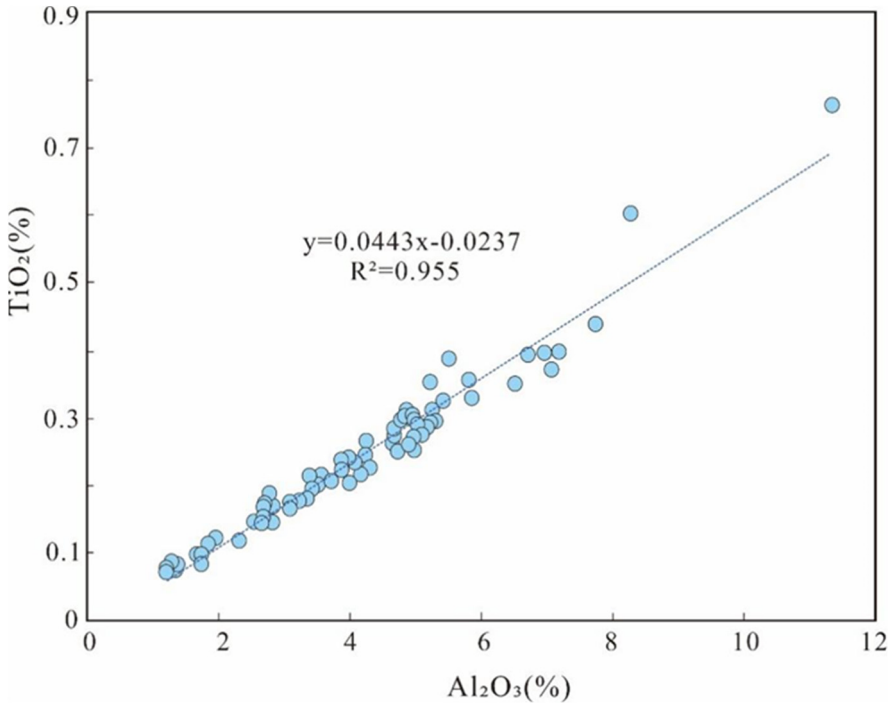

Figure 10. Correlation between TiO_2 and Al_2O_3 of fine-grained sedimentary rocks associated with Es3l–Es4u.

5. Discussion

5.1. Sedimentary Environment Evolution and Lithofacies Evolution Patterns

Through a detailed interpretation of the sedimentary environment and the distribution characteristics of different lithofacies, five primary stages of depositional environment evolution in the Es3l–Es4u of the Dongying Sag have been delineated (Figures 9 and 11).

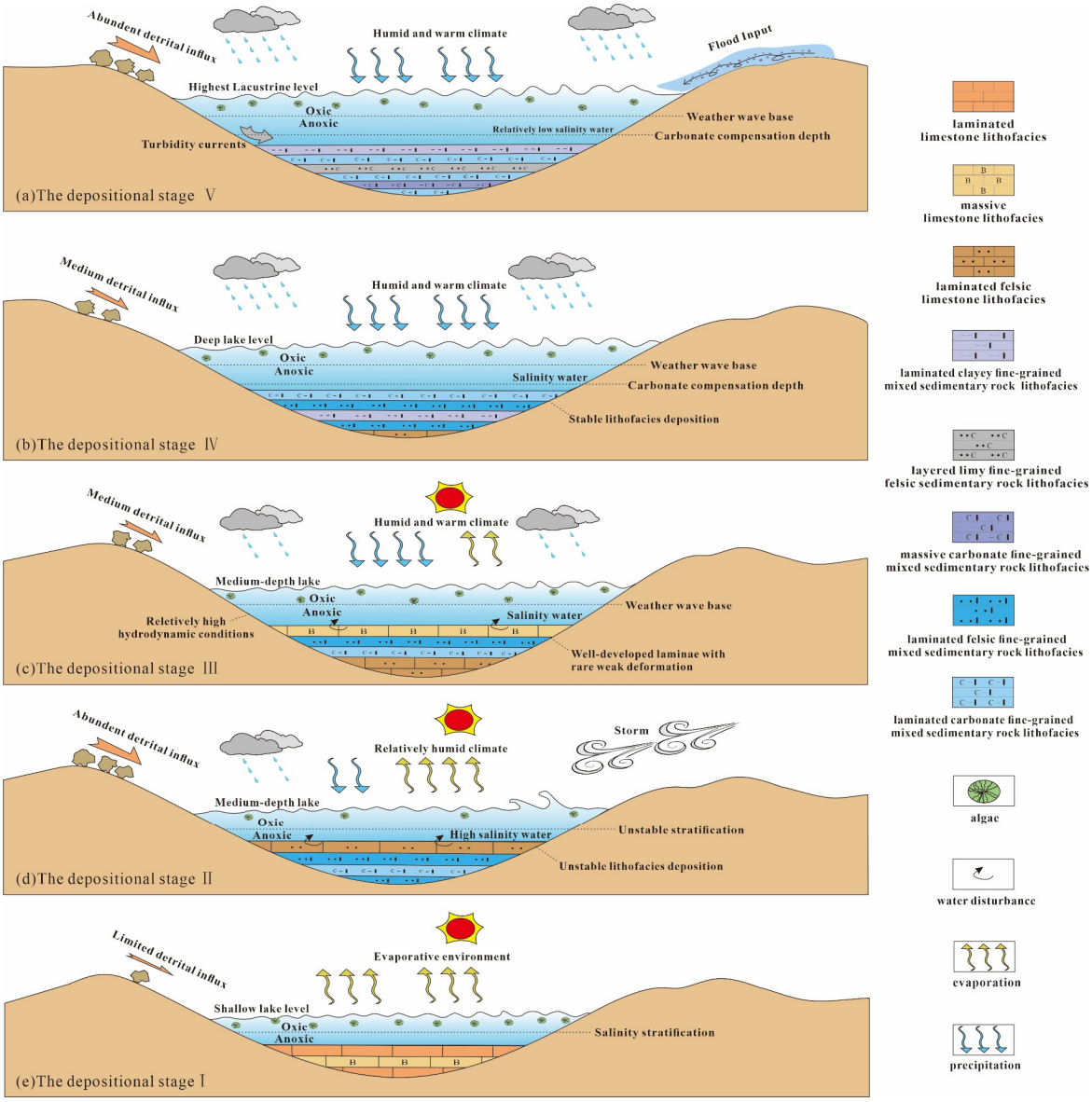

Figure 11. Depositional environment evolution in the Es3l–Es4u of the Shahejie Formation of the Dongying Sag, Bohai Bay Basin. (**a**) Depositional Stage I, (**b**) depositional Stage II, (**c**) depositional Stage III, (**d**) depositional Stage IV, (**e**) depositional Stage V.

5.1.1. Depositional Stage I

Sedimentary Stage I corresponds to the base of Es4u (3443 m~3390 m). Based on paleoenvironmental analysis, with proxies such as CIA (avg. 62.87), Ba (avg. 774.67μg), Sr/Ba (avg. 7.03), V/Sc (avg. 9.06), V/V + Ni (avg. 0.67), Al (avg. 3.02%), and Ti (avg. 0.17%), this period is characterized by an arid climate with intense evaporation. The lake basin was shallow with high salinity and minimal terrigenous detrital influx, indicating a hypersaline shallow lake environment (Figures 9 and 11).

Saline shallow lakes often have higher water temperatures in summer, along with sunlight that can penetrate the shallow waters, providing more opportunities for photosynthesis. This is conducive to biological reproduction, leading to higher productivity during this period. In contrast, the bottom waters are anoxic and highly saline. High salinity causes the stratification of the lake water [75], limiting exchange between layers and resulting in a strongly reducing environment, thereby enabling the better preservation of organic matter (TOC ranging from 0.56% to 2.83%, average 2.33%). During this stage, fine-grained sedimentary rocks developed laminated structures with contrasting light and dark laminae, a result of seasonal variations. In summer, carbonate components precipitate in the water due to biogeochemical activities, forming light calcite lamina. In winter, a large number of organisms die, and the suspended clay minerals and organic matter in the surface waters settle due to mechanical flocculation, forming dark laminae [76,77]. Due to the shallow nature of the lake and unstable hydrodynamic conditions, the lamination of the rocks during this stage shows significant undulations. The gray laminae often appear discontinuous, indicating turbulent water conditions during this stage. Primarily, ORLL developed, with intercalations of OMML or OPML, influenced by external factors including biological disturbances.

5.1.2. Depositional Stage II

Stage II corresponds to the middle part of Es4u (3390 m–3314 m), characterized by CIA (avg. 67.86), Ba (avg. 468.50μg), Sr/Ba (avg. 5.80), V/Sc (avg. 6.69), V/V + Ni (avg. 0.68), Al (avg. 5.28%), and Ti (avg. 0.32%). These values suggest a climate nearing humidity, with the deepening and gradual expansion of the lake basin, transitioning from a hypersaline shallow lake to a semi-deep lake environment (Figures 9 and 11).

This period is marked by a sharp decline in productivity and a significant increase in terrigenous influx, likely linked to frequent storm events. Previous research has highlighted the significant impact of West Pacific storms on the Es4u interval of the Dongying Sag [39,78]. Palynological studies suggest that an East Asian monsoon climate had already developed in Eastern China during the middle to late Eocene [79,80]. The Dongying Sag's geographic location during the Eocene, around 39° N latitude, positioned it between the winter storm belt and the summer typhoon belt (25°~45° latitude) [81,82], thus making it susceptible to the influences of the ancient East Asian monsoon [83], leading to frequent storm activities. Additionally, a global warming event from the early to middle Eocene also facilitated the formation of summer hurricanes (storm events) [78,84]. The sharp increase in terrigenous influx, reduction in the water body's reducing conditions, and strong fluctuations in geochemical proxies during this period (Figure 9) suggest a significant impact from intense storm activities.

These intense storms often disrupted the stratification of water bodies, stirring and suspending more terrigenous detrital and transporting them to deeper waters for deposition [85]. This led to a significant reduction in the water and a substantial increase in terrigenous influx. Consequently, the rock of this stage saw an increased content of felsic and clay minerals, significantly differing in mineral composition from Stage I. This stage primarily developed unevenly layered OMLFL, OMLFMR, and medium (to poor) organic-rich laminated gray fine-grained mixed sedimentary rocks. Additionally, storm-induced disturbances disrupted the reducing conditions and water flow at the lake bottom, making it difficult to preserve organic matter in the sediments (TOC content 0.54%~3.28%, avg. 1.78%) [86]. Lithofacies and thin section observations from this stage show wavy laminae, often with lenticular microcrystalline calcite, formed by the storm-induced disturbance that broke up weakly consolidated calcite laminae and deposited them in situ [87]. The disturbance caused by storms, disruptions in biological growth cycles, and increased terrigenous influx could significantly impact productivity, likely being the primary reason for the sharp decline in productivity during this stage.

5.1.3. Depositional Stage III

Stage III includes the upper part of Es4u and the base of Es3l (3314 m~3212 m). Geochemical proxies such as CIA (avg. 73.19), Ba (avg. 507.08 μg), Sr/Ba (avg. 4.70), V/Sc (avg. 9.35), V/V + Ni (avg. 0.67), Al (avg. 4.11%), and Ti (avg. 0.22%) suggest a shift to a humid climate during this period. The lake basin deepened and expanded, with stable terrigenous detrital influx, moderate organic productivity, and reducing conditions, indicative of a hypersaline semi-deep lake environment (Figures 9 and 11).

In the early phase of Stage III, the steady influx of terrigenous detrital into the lake basin, coupled with turbulent waters and lower paleoproductivity, led to a further deepening of the lake under the humid climate. Sediments deposited below the wave base formed thick OMLFL with significant lamination undulations. The dilution by freshwater continued to lower water salinity, increasing productivity. The reducing conditions of the water allowed for the better preservation of organic matter (an average TOC content of 2.38%). With an increased influx of terrigenous detrital, the lithofacies transitioned from limestone to fine-grained mixed sedimentary rocks, predominantly developing ORLCMR-1 and ORLFMR. The top part formed thick OMML due to short-term intense water disturbances.

5.1.4. Depositional Stage IV

Stage IV is located in the lower-middle part of the Es3l section (3212 m~3130 m). The geochemical proxies—CIA (avg. 74.99), Ba (avg. 534.73 μg), Sr/Ba (avg. 3.48), V/Sc (avg. 8.07), V/V + Ni (avg. 0.62), Al (avg. 3.45%), and Ti (avg. 0.20%) (Figures 9 and 11)—suggest an increasingly warm and humid climate. Terrigenous influx and salinity are slightly reduced compared to Stage III. This period is characterized by higher productivity and stronger water body reduction, indicative of an expansive semi-deep-to-deep lake environment. The overall stability and calmness of the lake basin environment during this stage are reflected by the gentle fluctuations of the geochemical proxies.

Compared to the predominance of OMLFL in Stage III, Stage IV almost entirely developed fine-grained mixed sedimentary rocks. This is believed to be associated with the continuous deepening of the lake body due to increased precipitation in a more humid climate, leading to an increase in terrigenous clastic influx and a reduction in early carbonate precipitation. This phenomenon can be understood using the concept of "Carbonate Compensation Depth (CCD)" from oceanography [50]. Carbonate precipitation depends on the relationship between the rate of carbonate production and dissolution, with the dissolution rate controlled by water depth. In sufficiently deep conditions within the lake basin, a CCD may form, below which carbonates tend to dissolve. During this period, the lake would predominantly receive ultra-fine-grained terrigenous detrital and clay minerals, leading to a gradual decrease in the proportion of carbonate minerals in the rocks.

Further reduction in water salinity allowed algae and other organisms to proliferate extensively, resulting in high lake productivity. This process, consuming oxygen in the water, further enhanced the reducing conditions in the deep waters at the lake bottom. The strong reducing conditions facilitated the excellent preservation of organic matter, with TOC showing high values (1.65%~4.2%, avg. 2.92%). In the lower part of this stage, the lake water depth might have been near the CCD, resulting in the interlayering of ORLFL and ORMFMR. As the water continued to deepen in the upper part, carbonate solubility increased and precipitation decreased, leading predominantly to the development of ORLFMR. The flat and continuous laminated structure of the rocks also reflects a profound and serene depositional environment, which stands in contrast to earlier stages.

5.1.5. Depositional Stage V

Stage V, located in the upper part of the Es3l section (3130 m~3030 m), is characterized by geochemical proxies CIA (avg. 76.94), Ba (avg. 592.56 μg), Sr/Ba (avg. 1.75), V/Sc (avg. 6.70), V/V + Ni (avg. 0.68), Al (avg. 4.96%), and Ti (avg. 0.29%) (Figures 9 and 11). The extensive development of pyrite in this stage reflects a paleoclimate that was very warm

and humid, with high productivity, strong reducing conditions, and a semi-saline-to-saline deep lake basin environment (Figures 9 and 11).

Similar to Stage IV, Stage V also experienced deep water conditions. The sedimentary structures of the lithofacies were primarily flat-laminated and massive. Continuous ORLCMR-1 developed extensively in the middle and lower parts. The lake level reached its highest point at the top of this stage, where the content of carbonate minerals was the lowest, and clay minerals precipitated through flocculation processes, leading to the development of ORLCMR-2, dominant in clay minerals.

Observations of the core revealed localized intercalations of sandy bands (Figure 6f), which we believe could be related to increased precipitation, causing intermittent flood events that brought a significant amount of terrigenous detrital into the lake basin. These sudden events sometimes suspended solid particles, including sand grains, forming turbidity currents that entered the deep-lake facies. Additionally, locally, there were small amounts of ORMCMR formed due to high deposition rates.

Overall, with the continual expansion and deepening of the lake basin, the study area from bottom to top shows a vertical distribution pattern of OMML, ORLL, OMLFL, ORLFMR, ORLCMR-1, to ORLCMR-2.

5.2. Influence of Sedimentary Environments on Lithofacies

5.2.1. Influence of Sedimentary Environments on Organic Matter Abundance

Sedimentary environments related to productivity and redox conditions play a crucial role in the accumulation and preservation of organic matter [8,88]. A depositional environment conducive to the aggregation and preservation of organic matter is a prerequisite for forming rocks rich in organic content. The accumulation and preservation of organic matter are influenced by multiple factors.

Firstly, paleoclimate is one of the key factors as it directly affects the species composition and distribution in water bodies, thereby impacting paleoproductivity [52,89]. Warm and humid climatic conditions are generally considered conducive to high-productivity environments, promoting the influx of organic matter [90]. Additionally, during dry climates when the basin's water supply is less than evaporation, the water body's salinity increases. The rise in water body mineralization due to higher salinity can cause water stratification, creating anoxic environments that are favorable for the preservation of organic matter. This is supported by the higher TOC in the relatively warm and humid Es3l compared to Es4u, as analyzed above. Paleo-redox conditions also play a significant role, where reducing environments help in the preservation of organic matter [91]. For example, in sedimentary Stage II, the decrease in the reducing nature of the water body led to the easier decomposition of organic matter, hence reflecting a decrease in TOC. The depth of a lake basin is an additional crucial factor, as deep lakes generally exhibit relatively stable water conditions conducive to the preservation of organic matter, while shallow lakes are more vulnerable to external disturbances that can lead to the decomposition of organic matter.

5.2.2. Influence of Sedimentary Structures on Lithofacies

The sedimentary structures of rocks primarily reflect the influence of lake basin depth and special event factors. In sedimentary Stage IV, it is evident that under calm and deep lake conditions, sedimentary rocks with flat-laminated structures are more prevalent, indicating a relatively stable depositional environment. Conversely, in Stages I and II, where the lake waters are shallower, the rocks are more susceptible to disturbances in the sedimentary environment, leading to more turbulent water conditions. Under such conditions, the rocks tend to develop non-planar lamination structures, lenticular laminated structures, or massive structures.

Special events, such as the intermittent flooding events in sedimentary Stage V, result in rapid sediment accumulation, forming massive structures. Thus, the sedimentary structures of rocks are closely related to the conditions of the lake waters and special events. By observing the sedimentary structures of rocks, we can glean critical information about

the paleoenvironment. These observations help us understand the dynamic processes that shaped the sedimentary record and provide insights into the ancient environmental conditions under which these rocks were deposited.

5.2.3. Influence of Sedimentary Environments on Mineral Components

The lithofacies composition is predominantly influenced by paleoclimate, terrigenous detrital influx, and lake depth, with paleoclimate being the most significant factor. Under arid and cold climatic conditions in the source region, the limited weathering processes lead to a diminished capacity of rivers to transport terrigenous detritus, resulting in water bodies that are comparatively pristine and enclosed. With evaporation exceeding precipitation, high salinity waters are formed, and under biogeochemical action, carbonate minerals precipitate at the lake bottom. Therefore, carbonate rocks are more developed in the Es4u sub-member.

As the climate gradually becomes warmer and more humid, weathering intensifies. Rivers carry a large amount of terrigenous detrital material into the lake, and as observed, the main rock type in Es3l transitions from limestone to fine-grained mixed sedimentary rock. This shift marks an increase in clastic and clay material, reflecting changes in sediment supply and climate.

Moreover, the content of carbonate in rocks is closely related to water depth. In Stages IV and V, as water bodies deepen and salinity is diluted, the concentration of CO_2^{2-} and Ca^{2+} ions in the water decreases, resulting in a reduction in the content of carbonate minerals in the rocks. Special sedimentary events, such as the storm events in sedimentary Stage II, significantly alter the size of terrigenous detrital influx and have a notable impact on the lithofacies composition. These dynamics are crucial for understanding the environmental changes and sedimentary processes that have occurred in the lake basin over geological time.

6. Conclusions

The Es3l–Es4u fine-grained sedimentary rocks in Dongying Sag are divided into 18 lithofacies types based on core and thin section observations, mineral content, and organic matter content analyses. These lithofacies are differentiated not only in mineral composition but also display significant variations in sedimentary structures and organic matter content. The predominant lithofacies include ORLL, OMML, OMLFL, ORLCMR-1, ORLFMR, and ORLCMR-2.

During the depositional period of the Es3l–Es4u interval in the Dongying Sag, the lake underwent various transitions, dividing the study area's depositional environment into five stages. Stage I corresponds to a saline shallow lake environment under arid climate conditions. Stage II had comparatively arid conditions, and the lake basin was influenced by frequent storm events. In Stage III, as the climate shifted from arid to humid, the lake basin gradually transitioned from a saline shallow lake to a semi-deep lake environment. During Stage IV, under more humid climatic conditions, the lake basin continued to expand, forming a wide range of saline, semi-deep-to-deep lake environments. Finally, in Stage V, under humid climatic conditions, the lake reached its maximum depth, developing into a semi-saline-to-saline deep lake environment.

The abundance of organic matter is primarily controlled by paleoproductivity and paleo-redox conditions. Warmer, more humid climates, suitable salinity, and deep-water environments are more conducive to the generation and preservation of organic matter. Changes in rock components are mainly influenced by paleoclimate. Under arid conditions, the formation of carbonate rocks is more significant, while humid conditions increase clastic material, leading to a transition from limestone to fine-grained mixed sedimentary rocks. The sedimentary structure of rocks is significantly influenced by lake depth. Flat-laminated structures are more likely to form in environments with deep and calm lake waters under humid climatic conditions, whereas shallower and disturbed waters under arid conditions tend to develop non-flat-laminated structures or massive structures. Moreover, special

sedimentary events, such as storm events and intermittent floods, can significantly affect the abundance of organic matter, rock components, and sedimentary structures by disturbing the water body and disrupting the reductive conditions at the lake bottom.

Author Contributions: Conceptualization, H.G.; methodology, H.G. and J.S.; validation, S.F., Z.L., L.C. and S.Y.; investigation, H.G., S.F. and Z.L.; data curation, S.F. and L.C.; writing—original draft, H.G.; writing—review & editing, J.S.; visualization, H.G. and Z.L.; supervision, J.S. and S.Y.; project administration, J.S.; funding acquisition, J.S. and H.G. All authors have read and agreed to the published version of the manuscript.

Funding: This study was supported by the National Natural Science Foundation of China (Grants 42102150) and National College Students Innovation and Entrepreneurship Training Program (No. 202311415039).

Data Availability Statement: Data are contained within the article.

Conflicts of Interest: The authors declare no conflicts of interest.

References

1. Krumbein, W.C. Shales and their environmental significance. *J. Sediment. Res.* **1947**, *17*, 101–108. [CrossRef]
2. Jiang, Z.X.; Duan, H.J.; Liang, C.; Wu, J.; Zhang, W.Z.; Zhang, J.G. Classification of hydrocarbon-bearing fine-grained sedimentary rocks. *J. Earth Sci.* **2017**, *28*, 693–976. [CrossRef]
3. Peng, J.; Yu, L.D.; Xu, T.Y.; Wang, Y.B.; Han, H.D. Analysis of Sedimentary Environment Conditions for Lacustrine Fine-Grained Sedimentary Rocks and Its Control of Lithofacies Development: A Case Study of the Lower Submember of Member 3 of Shahejie Formation in FY-1 Well, Dongying Sag, Bohai Bay Basin, China. *Geofluids* **2021**, *2021*, 6640706.
4. Abouelresh, M.O.; Slatt, R.M. Lithofacies and sequence stratigraphy of the Barnett Shale in east-central Fort Worth Basin, Texas. *AAPG Bull.* **2018**, *96*, 1–22. [CrossRef]
5. Wu, J.; Jiang, Z.X.; Tong, J.H.; Yang, L.; Li, J.; Nie, H.K. Sedimentary environment and control factors of fine-grained sedimentary rocks in the upper fourth Member of Paleogene Shahejie Formation, Dongying sag. *Acta Pet. Sin.* **2016**, *37*, 464.
6. Shi, J.Y.; Jin, Z.J.; Liu, Q.Y.; Huang, Z.K. Lithofacies classification and origin of the Eocene lacustrine fine-grained sedimentary rocks in the Jiyang Depression, Bohai Bay Basin, Eastern China. *J. Asian Earth Sci.* **2020**, *194*, 104002. [CrossRef]
7. Lazar, O.R.; Bohacs, K.M.; Macquaker, J.H.; Schieber, J.; Demko, T.M. Capturing key attributes of fine-grained sedimentary rocks in outcrops, cores, and thin sections: Nomenclature and description guidelines. *J. Sediment. Res.* **2015**, *85*, 230–246. [CrossRef]
8. Wang, G.P.; Jin, Z.J.; Hu, Z.Q.; Liu, G.X.; Zhu, T.; Du, W.; Wang, H.L.; Wu, Z. Sedimentary evolution characteristics of fine-grained lithofacies under the high-resolution isochronous shelf system: Insights from the wufeng-longmaxi shales in the sichuan basin. *Lithosphere* **2021**, *2021*, 20. [CrossRef]
9. Zhao, W.Z.; Zhu, R.K.; Hu, S.Y.; Hou, L.H.; Wu, S.T. Accumulation contribution differences between lacustrine organic-rich shales and mudstones and their significance in shale oil evaluation. *Pet. Explor. Dev. Zou* **2020**, *47*, 1160–1171. [CrossRef]
10. Guan, M.D.; Wu, S.T.; Hou, L.H.; Jiang, X.H.; Ba, D.; Hua, G.L. Paleoenvironment and chemostratigraphy heterogenity of the Cretaceous organic-rich shales. *Adv. Geo-Energy Res.* **2021**, *5*, 444–455. [CrossRef]
11. Khan, D.; Qiu, L.W.; Liang, C.; Mirza, K.; Rehman, S.U.; Han, Y.; Hannan, A.; Kashif, M.; Kra, K.L. Genesis and distribution of pyrite in the Lacustrine Shale: Evidence from the Es3x shale of the eocene shahejie formation, Zhanhua Sag, East China. *ACS Omega* **2021**, *7*, 1244–1258. [CrossRef] [PubMed]
12. Song, M.S.; Liu, H.M.; Wang, Y.; Liu, Y.L. Enrichment rules and exploration practices of Paleogene shale oil in Jiyang Depression, Bohai Bay Basin, China. *Pet. Explor. Dev. Online* **2020**, *47*, 242–253. [CrossRef]
13. Song, Y.; Cao, Q.; Li, S.F.; Hu, S.Z.; Zhu, K.; Ye, X.; Wan, L. Salinized lacustrine organic-rich shale influenced by marine incursions: Algal-microbial community, paleoenvironment and shale oil potential in the Paleogene Biyang Depression, East China. *Palaeogeogr. Palaeoclimatol. Palaeoecol.* **2021**, *580*, 110621. [CrossRef]
14. Li, J.J.; Liu, Z.; Zhang, X.W.; Feng, G.Q.; Liu, J.W.; Ma, Y.; Lu, S.F.; Li, W.H.; Zhou, N.W. Effects of paleoenvironment on continental shale oil enrichment and producibility in the Biyang depression. *AAPG Bull.* **2022**, *106*, 2043–2071. [CrossRef]
15. Tian, H.; He, K.; Huangfu, Y.H.; Liao, F.R.; Wang, X.M.; Zhang, S.C. Oil content and mobility in a shale reservoir in Songliao Basin, Northeast China: Insights from combined solvent extraction and NMR methods. *Fuel* **2024**, *357*, 129678. [CrossRef]
16. Tao, S.; Xu, Y.B.; Tang, D.Z.; Xu, H.; Li, S.; Chen, S.D.; Liu, W.B.; Cui, Y.; Gou, M.F. Geochemistry of the Shitoumei oil shale in the Santanghu Basin, Northwest China: Implications for paleoclimate conditions, weathering, provenance and tectonic setting. *Int. J. Coal Geol.* **2017**, *184*, 42–56. [CrossRef]
17. Milliken, K. Compositional Classification for Fine-Grained Sediments and Sedimentary Rocks: Foundation for Bulk Rock Property Prediction. In Proceedings of the AAPG Annual Convention and Exhibition, Denver, CO, USA, 31 May–3 June 2015.
18. Wang, G.C.; Carr, T.R. Organic-rich Marcellus Shale lithofacies modeling and distribution pattern analysis in the Appalachian Basin. *AAPG Bull.* **2013**, *97*, 2173–2205. [CrossRef]

19. Jiang, Y.Q.; Song, Y.T.; Qi, L.; Chen, L.; Tao, Y.Z.; Gan, H.; Wu, P.J.; Ye, Z.Y. Fine lithofacies of China's marine shale and its logging prediction: A case study of the Lower Silurian Longmaxi marine shale in Weiyuan area, southern Sichuan Basin, China. *Earth Sci. Front.* **2016**, *23*, 107–118. (In Chinese with English Abstract)
20. Loucks, R.G.; Ruppel, S.C. Mississippian Barnett Shale: Lithofacies and depositional setting of a deep-water shale-gas succession in the Fort Worth Basin, Texas. *AAPG Bull.* **2007**, *91*, 579–601. [CrossRef]
21. Simenson, A. Depositional Facies and Petrophysical Analysis of the Bakken Formation, Parshall Field, Mountrail County, North Dakota. Mines Thesis, Colorado School of Mines, Golden, CO, USA, 2010; pp. 1–221.
22. Zou, C.N.; Dong, D.Z.; Wang, S.J.; Li, J.Z.; Li, X.J.; Wang, Y.M.; Li, D.H.; Cheng, K.M. Geological characteristics and resource potential of shale gas in China. *Pet. Explor. Dev.* **2010**, *37*, 641–653. [CrossRef]
23. Liang, C.; Jiang, Z.X.; Yang, Y.T.; Wei, X.J. Characteristics of shale lithofacies and reservoir space of the Wufeng-Longmaxi Formation, Sichuan, Basin. *Pet. Explor. Dev.* **2012**, *39*, 691–698. (In Chinese with English Abstract) [CrossRef]
24. Jiang, Z.X.; Kong, X.X.; Yang, Y.P.; Zhang, J.G.; Zhang, Y.F.; Wang, L.; Yuan, X.D. Multi-source genesis of continental carbonate-rich fine-grained sedimentary rocks and hydrocarbon sweet spots. *Pet. Explor. Dev.* **2021**, *48*, 30–42. [CrossRef]
25. Ma, Y.Q.; Fan, M.J.; Lu, Y.C.; Liu, H.M.; Hao, Y.Q.; Xie, Z.H.; Li, P.; Du, X.B.; Hu, H.Y. Middle Eocene paleohydrology of the Dongying Depression in eastern China from sedimentological and geochemical signatures of lacustrine mudstone. *Palaeogeogr. Palaeoclimatol. Palaeoecol.* **2017**, *479*, 16–33. [CrossRef]
26. Pang, S.Y.; Cao, Y.C.; Liang, C. Lithofacies characteristics and sedimentary environment of Es4Uand Es3l: A case study of Well FY1 in Dongying sag, Bohai Bay Basin. *Oil Gas Geol.* **2019**, *40*, 799–809. (In Chinese with English Abstract)
27. Liu, Q.; Zeng, X.; Wang, X.J.; Cai, J.G. Lithofacies of mudstone and shale deposits of the Es3z-Es4s formation in Dongying sag and their depositional environment. *Mar. Geol. Quat. Geol.* **2017**, *37*, 147–156. (In Chinese with English Abstract)
28. Liang, C.; Wu, J.; Jiang, Z.X.; Cao, Y.C.; Song, G.Q. Sedimentary environmental controls on petrology and organic matter accumulation in the upper fourth member of the Shahejie Formation (Paleogene, Dongying depression, Bohai Bay Basin, China). *Int. J. Coal Geol.* **2018**, *186*, 1–13. [CrossRef]
29. Zhang, J.G.; Jiang, Z.X.; Liu, L.A.; Yuan, F.; Feng, L.Y.; Li, C.S. Lithofacies and depositional evolution of fine-grained sedimentary rocks in the lower submember of the Member 3 of Shahejie Formation in Zhanhua sag, Bohai Bay Basin. *Acta Pet. Sin.* **2021**, *42*, 293. (In Chinese with English Abstract)
30. Liu, H.M.; Yu, B.S.; Xie, Z.H.; Han, S.J.; Shen, Z.H.; Bai, C.Y. Characteristics and implications of micro-lithofacies in lacustrine-basin organic-rich shale: A case study of Jiyang depression, Bohai Bay Basin. *Acta Pet. Sin.* **2018**, *39*, 1328–1343. (In Chinese with English Abstract)
31. Chen, Z.H.; Huang, W.; Liu, Q.; Zhang, L.Y.; Zhang, S.C. Geochemical characteristics of the Paleogene shales in the Dongying depression, eastern China. *Mar. Pet. Geol.* **2016**, *73*, 249–270. [CrossRef]
32. Song, M.S. Sedimentary environment geochemistry in the Shasi section of southern ramp, Dongying depression. *J. Mineral. Petrol.* **2005**, *25*, 67–73.
33. Li, Y.; Li, Z.X.; Wang, D.D.; Song, G.Z.; Lv, D.W.; Yin, L.S.; Liu, H.Y.; Xu, C.H.; Kong, F.F.; Han, Q.Y. Continental lacustrine fine-grained lithofacies, assemblage and geological significance of unconventional petroleum: A case study of the Paleogene of the 4th member of the Shahejie formation in the Jiyang depression. *Energy Explor. Exploit.* **2023**, *41*, 62–83. [CrossRef]
34. Ye, H.; Shedlock, K.M.; Hellinger, S.J.; Sclater, J.G. The North China Basin: An example of a Cenozoic rifted intraplate basin. *Tectonics* **1985**, *4*, 153–169. [CrossRef]
35. Liu, C.L.; Wang, P.X. The role of algal blooms in the formation of lacustrine petroleum source rocks—Evidence from Jiyang depression, Bohai Gulf Rift Basin, eastern China. *Palaeogeogr. Palaeoclimatol. Palaeoecol.* **2013**, *388*, 15–22. [CrossRef]
36. Ding, L.; Xu, Q.; Yue, Y.H.; Wang, H.Q.; Cai, F.L.; Li, S. The Andean-type gangdese mountains: Paleoelevation record from the paleocene–eocene linzhou basin. *Earth Planet. Sci. Lett.* **2014**, *392*, 250–264. [CrossRef]
37. Zhao, L.; Li, L. The extensional pattern and dynamics of Bohai Bay basin in Late Mesozoic-Cenozoic. *Geol. China* **2016**, *43*, 470–485.
38. Li, L.; Zhong, D.L.; Shi, M.X. Cenozoic uplifting/subsidence coupling between the west Shandong Rise and the Jiyang Depression, northern China. *Acta Geol. Sin.* **2007**, *81*, 1215–1228.
39. Liang, C.; Jiang, Z.X.; Cao, Y.C.; Wu, J.; Wang, Y.S.; Hao, F. Sedimentary characteristics and origin of lacustrine organic-rich shales in the salinized Eocene Dongying Depression. *GSA Bull.* **2018**, *130*, 154–174. [CrossRef]
40. Wang, J.F. Sedimentary facies of the Shahejie formation of Paleogene in Dongying sag, Jiyang depression. *J. Palaeogeogr.* **2005**, *7*, 45–58.
41. Sheng, W.B.; Cao, Y.C.; Liu, H.; Zhang, Y. Evolutionary characteristics of the Palaeogene basin controlling boundary faults and types of basin architectures in the Dongying Depression. *Oil Gas Geol.* **2008**, *29*, 290–296. (In Chinese with English abstract)
42. Zhu, G.Y.; Jin, Q. Geochemical characteristics of two sets of excellent source rocks in Dongying Depression. *Acta Sedimentol. Sin.* **2003**, *21*, 506–512.
43. Li, S.M.; Pang, X.Q.; Li, M.W.; Jin, Z.J. Geochemistry of petroleum systems in the Niuzhuang South Slope of Bohai Bay Basin—Part 1: Source rock characterization. *Org. Geochem.* **2003**, *34*, 389–412. [CrossRef]
44. Wei, Z.F.; Zou, Y.R.; Cai, Y.L.; Wang, L.; Luo, X.R.; Peng, P.A. Kinetics of oil group-type generation and expulsion: An integrated application to Dongying Depression, Bohai Bay Basin, China. *Org. Geochem.* **2012**, *52*, 1–12. [CrossRef]

45. *SY-T 5163-2018*; Methods of X-ray Diffraction Analysis of Clay Minerals and Common Non-Clay Minerals in Sedimentary Rocks. China National Petroleum Corporation: Beijing, China, 2018.
46. *GB/T 19145-2022*; Determination of Total Organic Carbon in Sedimentary Rocks. China National Petroleum Corporation: Beijing, China, 2022.
47. *GB/T 14506.30-2010*; Methods for Chemical Analysis of Silicate Rocks-Part 30: Determination of 44 Elements. Standards Press of China: Beijing, China, 2010.
48. Peng, J.; Zeng, Y.; Yang, Y.M.; Yu, L.D.; Xu, T.Y. Discussion on classification and naming scheme of fine-grained sedimentary rocks. *Pet. Explor. Dev.* **2022**, *49*, 121–132. [CrossRef]
49. Zhang, S.; Chen, S.Y.; Cui, S.Z.; Gong, W.L.; Yu, J.Q.; Yan, J.H.; Shao, P.C.; Liu, Y. Characteristics and types of fine-grained sedimentary rocks lithofacies in semi-deep and deep lacustrine, Dongying Sag. *J. China Univ. Pet.* **2014**, *38*, 9–17.
50. Liu, H.; Liu, X.P.; Liu, G.Y.; Li, G.Y.; Wang, J.W.; Gao, Y.L.; Sun, B.; Hou, J.K.; Liu, H.X.; Sun, X.J. Sedimentary environment controls on the lacustrine shale lithofacies: A case study from the Nanpu depression, Bohai Bay Basin. *Geoenergy Sci. Eng.* **2023**, *225*, 211704. [CrossRef]
51. Yan, K.; Wang, C.L.; Mischke, S.; Wang, J.Y.; Shen, L.J.; Yu, X.C.; Meng, L.Y. Major and trace-element geochemistry of Late Cretaceous clastic rocks in the Jitai Basin, southeast China. *Sci. Rep.* **2021**, *11*, 13846. [CrossRef] [PubMed]
52. Rieu, R.; Allen, P.A.; Plötze, M.; Pettke, T. Climatic cycles during a Neoproterozoic "snowball" glacial epoch. *Geology* **2007**, *35*, 299–302. [CrossRef]
53. Nesbitt, H.; Young, G.M. Early Proterozoic climates and plate motions inferred from major element chemistry of lutites. *Nature* **1982**, *299*, 715–717. [CrossRef]
54. McLennan, S.M.; Hemming, S.; McDaniel, D.K.; Hanson, G.N. *Geochemical Approaches to Sedimentation, Provenance, and Tectonics*; Special Papers-Geological Society of America: Boulder, CA, USA, 1993; ISBN 978-081-372-284-9.
55. Ma, D.; Zhang, Z.J.; Zhou, C.M.; Cheng, D.W.; Hong, H.T.; Meng, H.; Yu, X.H.; Peng, Z.X. Element Geochemical Characteristics and Geological Significance of Mudstones from the Middle Jurassic Shaximiao Formation in Sichuan Basin, Southwest China. *ACS Omega* **2023**, *8*, 29979–30000. [CrossRef] [PubMed]
56. Wu, J.; Jiang, Z.X.; Wang, X. Sequence stratigraphy characteristics of lacustrine fine-grained sedimentary rocks: A case study of the upper fourth member of Paleogene Shahejie Formation, Dongying Sag, Bohai Bay Basin. *Nat. Gas Geosci.* **2018**, *29*, 5.
57. Lin, Z.K.; Zhang, S.L.; Li, C.H.; Wang, M.; Yan, J.P.; Cai, J.G.; Geng, B.; Hu, Q.H. Types of shale lithofacies assemblage and its significance for shale oil exploration: A case study of Shahejie Formation in Boxing Sag. *Pet. Reserv. Eval. Dev.* **2023**, *13*, 39–51, (In Chinese with English Abstract).
58. Dymond, J.; Suess, E.; Lyle, M. Barium in deep-sea sediment: A geochemical proxy for paleoproductivity. *Paleoceanography* **1992**, *7*, 163–181. [CrossRef]
59. Cao, Z.M.; Li, Y.T.; Rao, X.T.; Yu, Y.; Hathorne, E.C.; Siebert, C.; Dai, M.H.; Frank, M. Constraining barium isotope fractionation in the upper water column of the South China Sea. *Geochim. Cosmochim. Acta* **2020**, *288*, 120–137. [CrossRef]
60. Martinez-Ruiz, F.; Jroundi, F.; Paytan, A.; Guerra-Tschuschke, I.; Abad, M.D.M.; González-Muñoz, M.T. Barium bioaccumulation by bacterial biofilms and implications for Ba cycling and use of Ba proxies. *Nat. Commun.* **2018**, *9*, 1619. [CrossRef] [PubMed]
61. Fang, R.; Jiang, Y.Q.; Sun, S.S.; Luo, Y.; Qi, L.; Dong, D.Z.; Lai, Q.; Luo, Y.Z.; Jiang, Z.Z. Controlling factors of organic matter accumulation and lacustrine shale distribution in Lianggaoshan Formation, Sichuan Basin, SW China. *Front. Earth Sci.* **2023**, *11*, 1218215. [CrossRef]
62. Kong, X.X.; Jiang, Z.X.; Zheng, Y.H.; Xiao, M.; Chen, C.; Yuan, H.; Chen, F.L.; Wu, S.Q.; Zhang, J.G.; Han, C.; et al. Organic geochemical characteristics and organic matter enrichment of mudstones in an Eocene saline lake, Qianjiang Depression, Hubei Province, China. *Mar. Pet. Geol.* **2020**, *114*, 104194. [CrossRef]
63. Xu, S.; Wang, Y.X.; Bai, N.; Wu, S.Q.; Liu, B.C. Organic matter enrichment mechanism in saline lacustrine basins: A review. *Geol. J.* **2023**, *59*, 155–168. [CrossRef]
64. Hou, H.H.; Shao, L.Y.; Li, Y.H.; Liu, L.; Liang, G.D.; Zhang, W.L.; Wang, X.T.; Wang, W.C. Effect of paleoclimate and paleoenvironment on organic matter accumulation in lacustrine shale: Constraints from lithofacies and element geochemistry in the northern Qaidam Basin, NW China. *J. Pet. Sci. Eng.* **2022**, *208*, 109350. [CrossRef]
65. Fan, D.J.; Shan, X.L.; Makeen, Y.M.; He, W.T.; Su, S.Y.; Wang, Y.B.; Yi, J.; Hao, G.L.; Zhao, Y.T. Response of a continental fault basin to the global OAE1a during the Aptian: Hongmiaozi Basin, Northeast China. *Sci. Rep.* **2021**, *11*, 7229. [CrossRef] [PubMed]
66. Zhao, Z.R.; Dong, C.M.; Ma, P.J.; Lin, C.Y.; Li, G.A.; Du, X.Y.; Luan, G.Q.; He, Y.J.; Liu, W.B. Origin of Dolomite in Lacustrine Organic-Rich Shale: A Case Study in the Shahejie Formation of the Dongying Sag, Bohai Bay Basin. *Front. Earth Sci.* **2022**, *10*, 909107. [CrossRef]
67. Yin, J.; Wang, Q.; Hao, F.; Guo, L.X.; Zou, H.Y. Palaeoenvironmental reconstruction of lacustrine source rocks in the lower 1st Member of the Shahejie Formation in the Raoyang Sag and the Baxian Sag, Bohai Bay Basin, eastern China. *Palaeogeogr. Palaeoclimatol. Palaeoecol.* **2018**, *495*, 87–104. [CrossRef]
68. Khan, D.; Liu, Z.J.; Qiu, L.W.; Liu, K.Y.; Yang, Y.Q.; Nie, C.; Liu, B.; Xin, L.; Habulashenmu, Y. Mineralogical and geochemical characterization of lacustrine calcareous shale in Dongying Depression, Bohai Bay Basin: Implications for paleosalinity, paleoclimate, and paleoredox conditions. *Geochemistry* **2023**, *83*, 125978. [CrossRef]

69. Zhou, C.; Jiang, S.Y. Palaeoceanographic redox environments for the lower Cambrian Hetang Formation in South China: Evidence from pyrite framboids, redox sensitive trace elements, and sponge biota occurrence. *Palaeogeogr. Palaeoclimatol. Palaeoecol.* **2009**, *271*, 279–286. [CrossRef]
70. Hua, J.C.; Zhu, X.L.; Feng, L.J.; Huang, J. Progressive oxidation of anoxic and ferruginous deep-water during deposition of the terminal Ediacaran Laobao Formation in South China. *Palaeogeogr. Palaeoclimatol. Palaeoecol.* **2012**, *321*, 80–87.
71. Liu, H.M.; Wang, Y.; Yang, Y.H.; Zhang, S. Sedimentary Environment and Lithofacies of Fine-Grained Hybrid Sedimentary in Dongying Sag: A Case of Fine-Grained Sedimentary System of the Es4. *Earth Sci.* **2020**, *45*, 3543–3555. (In Chinese with English Abstract)
72. Rimmer, S.M. Geochemical paleoredox indicators in Devonian–Mississippian black shales, central Appalachian Basin (USA). *Chem. Geol.* **2004**, *206*, 373–391. [CrossRef]
73. Govin, A.; Holzwarth, U.; Heslop, D.; Ford Keeling, L.; Zabel, M.; Mulitza, S.; Collins, J.; Chiessi, C.M. Distribution of major elements in Atlantic surface sediments (36°N–49°S): Imprint of terrigenous input and continental weathering. *Geochem. Geophys. Geosystems* **2012**, *13*, 1. [CrossRef]
74. Di Leo, P.; Dinelli, E.; Mongelli, G.; Schiattarella, M. Geology and geochemistry of Jurassic pelagic sediments, Scisti silicei Formation, southern Apennines, Italy. *Sediment. Geol.* **2002**, *150*, 229–246. [CrossRef]
75. Kong, X.X.; Jiang, Z.X.; Ju, B.S.; Liang, C.; Cai, Y.; Wu, S.Q. Fine-grained carbonate formation and organic matter enrichment in an Eocene saline rift lake (Qianjiang Depression): Constraints from depositional environment and material source. *Mar. Pet. Geol.* **2022**, *138*, 105534. [CrossRef]
76. Liu, S.J.; Cao, Y.C.; Liang, C. Lithologic characteristics and sedimentary environment of fine-grained sedimentary rocks of the Paleogene in Dongying sag, Bohai Bay Basin. *J. Palaeogeogr.* **2019**, *21*, 479–489, (In Chinese with English Abstract).
77. Liu, B.; Song, Y.; Zhu, K.; Su, P.; Ye, X.; Zhao, W.C. Mineralogy and element geochemistry of salinized lacustrine organic-rich shale in the Middle Permian Santanghu Basin: Implications for paleoenvironment, provenance, tectonic setting and shale oil potential. *Mar. Pet. Geol.* **2020**, *120*, 104569. [CrossRef]
78. Wang, J.H.; Jiang, Z.X.; Zhang, Y.F. Subsurface lacustrine storm-seiche depositional model in the Eocene Lijin Sag of the Bohai Bay Basin, East China. *Sediment. Geol.* **2015**, *328*, 55–72. [CrossRef]
79. Chen, Q.; Liu, Y.S.; Utescher, T. Eocene monsoon prevalence over China: A paleobotanical perspective. *Palaeogeogr. Palaeoclimatol. Palaeoecol.* **2012**, *365*, 302–311.
80. Song, S.; Tang, Z.H.; Xi, D.P.; Yang, S.L. Palynology-based reconstructions for climatic patterns in the Eocene–Oligocene of eastern Asia: Implications of the monsoonal circulation history. *J. Asian Earth Sci.* **2023**, *257*, 105836. [CrossRef]
81. Boucot, A.J.; Chen, X.; Scotese, C.R.; Fan, J.X. *The World Paleoclimate Reconstruction in Phanerozoic*; SEPM Society for Sedimentary Geology: Claremore, OK, USA, 2009; ISBN 978-156-576-289-3.
82. Marsaglia, K.M.; Klein, G.D. The paleogeography of Paleozoic and Mesozoic storm depositional systems. *J. Geol.* **1983**, *91*, 117–142. [CrossRef]
83. Huber, M.; Goldner, A. Eocene monsoons. *J. Asian Earth Sci.* **2012**, *44*, 3–23. [CrossRef]
84. Pagani, M.; Zachos, J.C.; Freeman, K.H.; Tipple, B.; Bohaty, S. Marked decline in atmospheric carbon dioxide concentrations during the Paleogene. *Science* **2005**, *309*, 600–603. [CrossRef] [PubMed]
85. Palanques, A.; Puig, P.; Guillén, J.; Durrieu de Madron, X.; Latasa, M.; Scharek, R.; Martín, J. Effects of storm events on the shelf-to-basin sediment transport in the southwestern end of the Gulf of Lions (Northwestern Mediterranean). *Nat. Hazards Earth Syst. Sci.* **2011**, *11*, 843–850. [CrossRef]
86. Zhang, C.C.; Fang, C.G.; Huang, Z.Q.; Zhou, D.R.; Liu, T. Sedimentary characteristics of the Early Silurian storm deposits and the effect of storms on shale properties in the Lower Yangtze Region. *Nat. Gas Geosci.* **2022**, *33*, 1585–1596.
87. Peng, J.; Xu, T.Y.; Yu, L.D. Sedimentary characteristics and controlling factors of lacustrine fine-grained rocks of the fourth member of Shahejie formation in Dongying depression. *Lithol. Reserv.* **2020**, *32*, 1–11.
88. Li, S.Z.; Liu, X.F.; Cen, C.; Yang, S.C.; Xiao, E.Z.; Zhang, X.T.; He, W.H.; Liu, L.X. Sedimentary paleoenvironment and organic matter accumulation model of the Lower Silurian Gaojiabian Formation shales in the Lower Yangtze region, South China. *Geoenergy Sci. Eng.* **2023**, *221*, 211347. [CrossRef]
89. Nesbitt, H.W.; Young, G.M.; McLennan, S.M.; Keays, R.R. Effects of chemical weathering and sorting on the petrogenesis of siliciclastic sediments, with implications for provenance studies. *J. Geol.* **1996**, *104*, 525–542. [CrossRef]
90. Chen, G.; Gang, W.Z.; Chang, X.C.; Wang, N.; Zhang, P.F.; Cao, Q.Y.; Xu, J.B. Paleoproductivity of the Chang 7 unit in the Ordos Basin (North China) and its controlling factors. *Palaeogeogr. Palaeoclimatol. Palaeoecol.* **2020**, *551*, 109741. [CrossRef]
91. Li, C.; Chen, S.J.; Liao, J.B.; Hou, Y.T.; Yu, J.; Liu, G.L.; Xu, K.; Wu, X.T. Geochemical characteristics of the chang 7 member in the southwestern ordos basin, China: The influence of sedimentary environment on the organic matter enrichment. *Palaeoworld* **2023**, *32*, 429–441. [CrossRef]